IRE Transactions

IEEE

ON AUTOMATIC CONTROL

PGAC-3 **NOVEMBER, 1957**

TABLE OF CONTENTS

PUBLISHED BY THE

PROFESSIONAL GROUP ON AUTOMATIC CONTROL

IRE PROFESSIONAL GROUP ON AUTOMATIC CONTROL

The Professional Group on Automatic Control is an organization, within the framework of the IRE, of members with principal professional interest in Automatic Control. All members of the IRE are eligible for membership in the Group and will receive all Group publications upon payment of prescribed assessments.

Annual Assessment: $2.00

IRE TRANSACTIONS®
on Automatic Control

George S. Axelby, *Editor*, Air Arm Division, Westinghouse Electric Corp., Box 746, Baltimore, Md.

Published by the Institute of Radio Engineers, Inc., for the Professional Group on Automatic Control, 1 East 79th Street, New York 21, New York. Responsibility for the contents rests upon the authors, and not upon the IRE, the Group or its members. Individual copies available for sale to IRE-PGAC members at $1.10, to IRE members at $1.65 and to nonmembers at $3.30.

PGAC TRANSACTIONS Policies

It may be noted that some of the papers in this issue were originally conceived over a year ago. Four of them were presented in preliminary form at WESCON in 1956. This long delay between conception and publication was partly due to our policy of having potential papers criticized by several reviewers. Their comments were edited and returned to the authors with suggestions for revising the papers.

Most of the reviewers have been prompt in commenting on the papers—although a few have never responded. However, all of the cooperative reviewers of automatic control papers have been particularly critical as they are instructed to be. In fact, the main purpose of the reviews is to eliminate papers which are not well written, or are not contributions to the control field. The papers may be tutorial, they may discuss an application of theory to the control system, or they may concern an entirely new development in the field. In any case, the PGAC hopes to establish a reputation for publishing papers of high quality.

Ordinarily, a paper is returned to the author only once, but if it is a tutorial paper, or if a major change is recommended in a potentially worthwhile paper, it may be returned to the author more than once. This causes a delay in the publication of the paper, but if it improves the quality of the paper and makes it more useful, we believe that the delay is justified.

In the future, when the list of competent reviewers grows longer and the editorial procedure becomes more efficient, the delay between the receipt of papers and their publication will be shorter.

A list of current reviewers is given in this issue. Anyone who is interested in keeping pace with recent progress in his special field by reviewing papers will be included in future lists if he will send his name to the PGAC TRANSACTIONS editor and state his particular interest. Of course, reviewers, as well as any other contributors, are urged to submit their own papers for future publication. New papers concerning any phase of automatic control are always welcome, particularly if they are concerned with over-all control system concepts. It is hoped that many potential papers will be conceived at local PGAC chapter meetings and reported to the TRANSACTIONS editor.

It should be noted that special TRANSACTIONS may contain papers which have not been reviewed. These TRANSACTIONS will include only those papers presented at PGAC sponsored symposia or conferences. This is the procedure similar to that followed by the IRE editorial department: papers in the PROCEEDINGS are reviewed, but those published in the NATIONAL CONVENTION RECORD and WESCON CONVENTION RECORD are not. Parts of each of these Records will be distributed to PGAC members each year in addition to the regular PGAC TRANSACTIONS, special TRANSACTIONS, Newsletters, and Bulletins.

Tentatively, two regular PGAC TRANSACTIONS with reviewed papers are to be issued each year. The spring issue will contain a PGAC membership directory, a registry of those who identify themselves professionally with the automatic control field. Particular months for the publications may be scheduled after the flow of incoming papers is more consistent. In the future it is hoped that the TRANSACTIONS will improve in quality and increase in quantity as our Professional Group develops.

—*The Editor.*

The Issue in Brief

As in the previous TRANSACTIONS, the papers included here are varied in nature and in scope.

The first paper is an easily read discussion with no mathematics. The second concerns an application of the describing function method and its relation to the root locus of a missile system. Root loci are reviewed and related to pulsed-data systems in the next paper, and the theme of pulsed data is continued in the fourth paper where multirate switches are used and the mathematics becomes more predominate. Mathematics is used extensively in the last two papers which are concerned with statistical properties and optimization of control systems.

A brief review of each paper follows.

Analog or Digital Computer for Process Control?, **T. M. Stout**—Page 3

This is an excellent introduction to process control and its associated problems which are quite different from those found in the frequently discussed machine tool or fire control systems. One of the several problems, the choice of an analog or digital computer, is treated in detail with respect to use, versatility, flexibility, precision, accuracy, speed cost, and reliability. Examples of analog and digital computer applications in process control are given.

Analysis of a Nonlinear Control System for Stabilizing a Missile, **Leonard Atran**—Page 8

The describing function technique is used to determine graphically the relationship among frequency, hysteresis band, and system time delays in a missile roll control servoutilizing peripheral, tangentially operating jets.

Relationships governing angular position and rates are found to be functions of a steady-state oscillating frequency, control full magnitude, and missile constants. A comparison is made between the root locus and amplitude-phase presentation, and an analog computer study is discussed.

Root Locus Method of Pulse Transfer Function for Sampled-Data Control Systems, **Masahiro Mori**—Page 13

The original Japanese version of this paper was published in *Automatic Control* (*Japan*) in 1955. Translational difficulties, reviews, and rewriting at a distance have delayed the publication of the paper in the United States. In the meantime, papers by G. W. Johnson, D. P. Lindorff, C. G. A. Nordling, E. I. Jury, and J. G. Truxal have discussed root loci of sampled data systems in American publications. Professor Mori's paper has been included to illustrate the original contribution to automatic control which was done in Japan and to present a useful review, with examples, of the relationships between the root loci in the s and z planes for continuous and sample data systems.

Input-Output Analysis of Multirate Feedback Systems, **George M. Kranc**—Page 21

A general analytical technique described in this paper permits the extension of z transform methods to sampled data systems containing synchronized switches which do not operate with the same sampling rate. These systems are referred to as multirate sampling systems.

Multirate sampling is used for purely computational purposes, for converting data in some flight control systems, or for system compensation to improve performance.

Statistical Design and Analysis of Multiply-Instrumented Control Systems, **Robert M. Stewart**—Page 29

Wiener's least-square filter theory is applied to common types of multiply instrumented control systems. Multiply instrumented control systems are those in which more than one sensing instrument is used such as a radar or communications system using frequency diversity, inertial guidance systems using accelerometer, velocity, and position data, or a multivariable process control system.

A Time Domain Synthesis for Optimum Extrapolators, **Carl W. Steeg, Jr.**—Page 32

This paper includes considerable mathematical background fundamental to time domain synthesis which can be useful to control engineers interested in the design of optimum predictors and the study of certain nonlinear systems. Because the techniques are new to most control engineers, the mathematics alone may provide a challenging and useful study. An example at the end of the paper aids in understanding the method.

The method is a direct solution of the integral equation for the optimum predictor in terms of the solution to the integral equation for the optimum filter, and it circumvents practical difficulties found in the techniques derived by Wiener. A procedure is given for avoiding the solution of the integral equations in the synthesis of the optimum extrapolator.

The synthesis procedure simplifies extrapolator designs which are used when the prediction interval is a nonnegative time function instead of a prediction interval that is always a fixed future time from a continuously varying instant.

Analog or Digital Computer for Process Control?*

T. M. STOUT†

Summary—**Although much has been written about the push-button or computer-controlled factory, there has been little discussion of the relative merits of analog and digital computers for control applications. Engineers familiar with computers are aware of the advantages and disadvantages of analog and digital computers as tools for scientific investigations. They have probably not considered their suitability for process control applications. In this paper, we will:**

1) Outline some of the tasks that will probably be assigned to a process control computer;
2) State some of the questions that must be answered before any computer is selected;
3) Review some of the characteristics of analog and digital computers with special reference to process control requirements;
4) Describe some systems already installed or about to be installed, in which computers are used.

Following this discussion, it will be evident, as might be anticipated in advance, that each type of computer has characteristics which make it preferable for particular kinds of applications. Analog computers are fast, simple, and inexpensive for relatively small control jobs, while digital computers have accuracy, versatility, and flexibility which adapt them to more complex control jobs.

Introduction

Fields of Application

THE kind of application and the role assigned to the computer make quite a difference in the characteristics that the control computer should have. The applications that we have in mind, as we approach the comparison of analog and digital computers, are found in the chemical, petroleum, and related industries such as metals, drugs, cement, soap, and paper manufacturing.

The common characteristic of these industries is their use of chemical and physical processes on essentially continuous streams of raw materials.

This paper does not discuss the application of computers or computer-like equipment for machine tool control or operation of automatic assembly machines. These applications seem to involve a different set of design considerations and are receiving attention elsewhere.

The Role of the Computer

For plants of the type we are considering, we can visualize a system having the general form shown in Fig. 1. This picture, used in various forms by many authors, shows a process of some kind which takes in raw materials, chemicals, water and energy in various forms (such as electricity, steam, gas, or fuel oil). By a combination of steps, a number of products or by-products are made, and some waste is created.

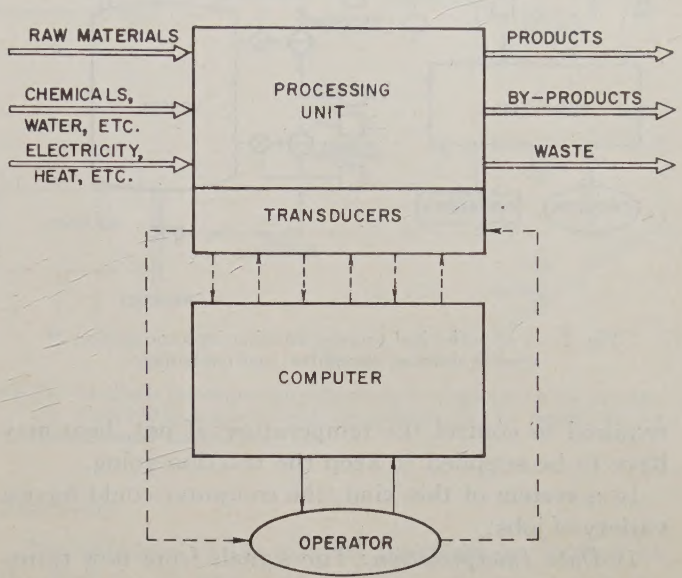

Fig. 1—Schematic diagram of a computer control system.

Control of a plant like this is now exercised by measuring flow rates, pressures, temperatures, levels, and other quantities which characterize the state of the process. This information, in combination with composition data from laboratory analyses or on-line analyzers, is used to govern the operation of individual controllers at various points in the process. These controllers maintain the flow rates, pressures, temperatures, levels, and so on at values which are expected to produce the desired product in the best possible way. These values, or "set points," are established initially by the process designers and are modified as time goes on by the engineers and operators in charge of the process.

In the computer-controlled process of the future, the various measurements will be supplied to a computer through appropriate amplifiers and converters. Calculations and decisions leading to selection of the optimum set points will be made by the computer, and the results of its efforts will be transmitted back to the process. The operator will receive information about the process from the computer and can modify the operation of the computer or, in an emergency, he can exercise control as he does today by looking at recorders and manually changing the set points of the controllers.

Jobs for the Computer

To make things more specific, we may look at the hypothetical process shown in Fig. 2. In this process, a feed material is treated with a reagent (or two feed materials are combined) at elevated pressure and temperature in a vessel where a chemical reaction takes place. If the reaction is exothermic, a coolant will be

* Manuscript received by the PGAC, June 3, 1957.
† The Ramo-Wooldridge Corp., Los Angeles, Calif.

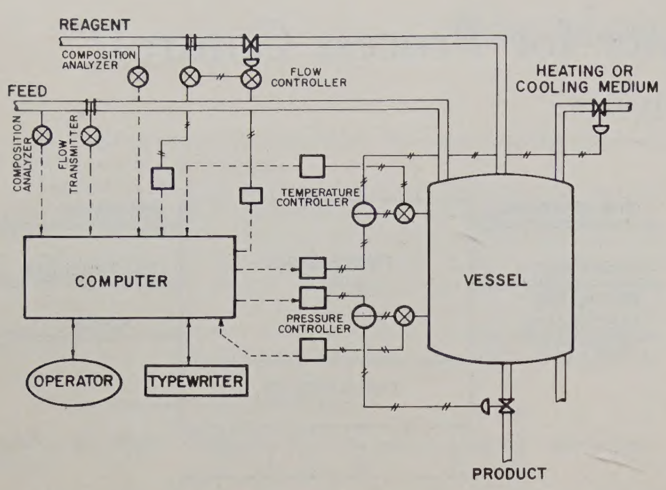

Fig. 2—A hypothetical process showing interconnection of sensing devices, computer, and controllers.

required to control the temperature; if not, heat may have to be supplied to keep the reaction going.

In a system of this kind, the computer could have a variety of jobs:

1) *Data Interpretation:* The signals from flow transmitters, thermocouples, and in fact, from any instrument, are not direct indications of the quantity being measured. Scale factors and calibration curves must be applied to obtain the desired information. At a minimum, the same treatment must be applied to the output of composition analyzers; in some cases, simultaneous equations must be solved to uncover the desired information.

2) *Mixing or Blending Calculations:* The flow rate of the reagent may require continuous adjustment in order to maintain a fixed ratio of reagent to the active component of the feed material in the face of variations in the feed rate or composition. Or, where the effectiveness of the reagent does not increase in direct proportion to the amount used, the optimum ratio might be a function of fluctuating material and product costs.

3) *Control of Reaction Conditions:* Because the product yield may drop off at very high feed rates, it may sometimes be advantageous to throw away part of the available feed. Raising the pressure by closing the valve at the outlet of the reactor might raise the yield while cutting down the feed rate. Raising the temperature might speed up the reaction but cut down the equilibrium yield. Where such optimum conditions result from the combined effects of technical and economic factors, the computer might keep the process operating continuously at the optimum points despite fluctuations in material feed rates and compositions, costs, environmental and equipment conditions, and so on.

In the case of batch operations, the computer might be used to enforce a rigid schedule of operations. More to the point, however, the computer might control the process in response to the actual progress of the reaction. In similar fashion, the computer might assist in starting and shutting down a continuous process.

4) *Data Processing:* The computer in a control system of this kind can be expected to perform some data processing or logging functions. Flow can be totalized or averaged for the accounting department, for example, and various computed quantities as well as basic process data can be made available to the process engineers.

5) *Diagnostic and Alarm Functions:* The computer should be designed to check the operation of the process, the measuring instruments, and the control system itself, with suitable alarm signals provided to the operator in the case of equipment malfunctions or breakdowns.

System Design

System Analysis

The example just discussed gives some idea of the kinds of things that can be done with a computer in process control. Exactly what can and, equally important, should be done and how to do it, must be established by a thorough study of the problem at hand. This study must answer such questions as:

- What are the objectives of the process?
- What are the raw materials and products involved? What are their characteristics, flow rates, and dollar values? What are the variations in these properties?
- What quantities can be measured? Controlled?
- What are the relations between the important quantities?
- Where are the equipment bottlenecks?
- What are the dynamic characteristics of the process and its equipment?
- Can the quantities necessary for improved control be measured with the requisite speed and accuracy?
- What kind of computer should be used? How should it be used?

After answering all of these questions, then it is necessary to draw up detailed specifications of the system components, specify their interconnections, outline operating procedures for regular and emergency conditions, and attend to a myriad of other details leading to the installation, test, and operation of the complete system.

Choice of Computer

The choice of an analog or digital computer, the subject of this paper, is therefore only one of the problems facing the control system designer. It would be a mistake to consider that there is a single answer to the question, "Analog or Digital Computers for Process Control?" and that this discussion will settle the problem for all time.

There is a children's book called "Are Dogs Better Than Cats?" which might provide the theme for the remainder of this paper. In the book, a boy says that cats can't swim, and a girl says dogs can't climb trees. After several pages of this sort of argument, they finally agree that "Dogs are better for dog things, and cats are

better for cat things." Much the same conclusion should be reached on the question of analog vs digital computers!

Use of Computer

The manner in which the computer will be used has an important bearing on its specifications. If the computer supervises conventional minor-loop controllers, as shown in Fig. 3(a), its tasks and requirements are quite different from those encountered if the computer acts directly upon the valves which govern the flow of materials and utilities, as shown in Fig. 3(b). In the first case, the instantaneous regulation of the process conditions is left to conventional feedback controllers of the kind now used for this purpose; the computer performs a supervisory function similar to that performed by the operator and process engineers. In the event of computer failure, control can return to the present manual mode. In the second case, the computer must be fast enough to keep pace with the disturbances affecting the process and reliable enough to remain on the job between scheduled maintenance periods.

Although the supervisory type of computer control leaves something to be desired in the way of equipment economy, it represents the probable course of development. We see little likelihood that the process industries will authorize the removal of conventional controllers and the substitution of presently untried control computers. This reading of the crystal ball affects our rankings of analog and digital computers in the discussion that follows. People with a different view of the future will perhaps arrive at a different ranking.

Computer Characteristics

In choosing between analog and digital computers, a wide variety of characteristics should be considered.[1] The following list contains the most important of these characteristics, with some comments on the relative standing of analog and digital computers. Some of the following remarks may be controversial, but others are, perhaps, pretty generally accepted.

Versatility

Digital computers can, in principle, perform any kind of calculation that can be specified by a sequence of arithmetic operations and yes-or-no decisions. Although we may concede that ingenious designers could develop an analog computer to perform any job that might be named, analog computers are best adapted to calculations involving the basic arithmetic and calculus operations of addition, subtraction, multiplication by constants, integration, and single-variable function generation. Multiplication of variables, generation of functions of several variables, and other complex operations can be performed, but less satisfactorily.

[1] M. Rubinoff, "Analog vs digital computers," Proc. IRE, vol. 41, pp. 1254–1262; October, 1953.

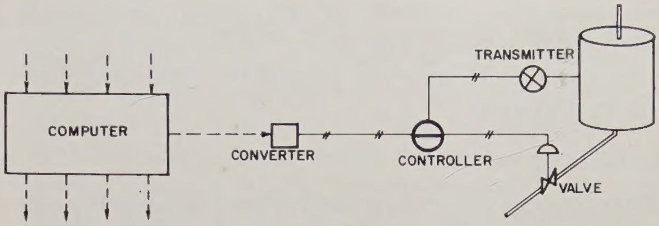

(a)

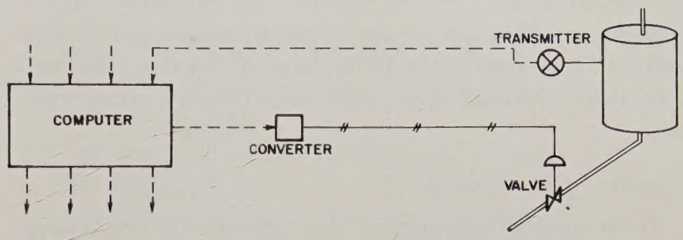

(b)

Fig. 3—Methods for connecting the control computer to the process: (a) supervising conventional controllers, (b) as substitute for conventional controllers.

Flexibility

Modification of the control functions performed by the digital computer requires only a change in the program. With an analog computer, such modifications may involve only changes of the interconnections between the elements, or they may mean large-scale substitution or addition of new computing elements.

Precision

The term "precision" denotes "sharpness of definition" and is related to the number of figures used to represent physical quantities in numerical form. Although the precision of digital computations can be extended at will, analog computer results can generally be read to only three or four figures. Either type is probably adequate for control use on this score.

Accuracy

The term "accuracy" denotes "correctness" or "conformity with truth." In a digital computer, inaccuracies arise from the necessity for approximate calculation schemes; in an analog computer, from inaccuracies or drifts in the calibration of its components. The digital computer can be made to give results as accurate as the original data, but additional errors will inevitably be introduced by analog computation.

Speed

The speeds of both types of computers are probably adequate for the kind of supervisory control of present processes described above. The digital computer is probably better equipped for very *slow* operations such as long-term integration or data storage, while the analog computer may have an edge for control of very high-speed processes.

Part of the speed advantage of analog computers stems from simultaneous or parallel operation of the

basic computing elements. If sequential operation is used in order to reduce the amount of equipment, either to cut costs or to improve reliability, this advantage tends to disappear.

Input-Output

Since most of the sensing devices used in present processes have analog outputs, the analog computer can be connected to the process without use of analog-digital converters. This advantage is not so significant if data will be converted anyway for digital logging and will diminish as digital sensing devices become more common.

Amount of Equipment

With analog computers, the amount of equipment needed is roughly proportional to the amount of computing to be done. With digital computers, on the other hand, a significant amount of equipment is needed to perform the first calculation, but the amount of equipment does not increase as rapidly with the amount of computing.

Cost

Because the cost depends heavily on the amount of equipment needed, it can be expected that analog computers will be less expensive when only a little computing must be done, and that the digital computer will have an edge for jobs requiring extensive computing. However, it is possible that analog computers will require more tailoring to fit particular jobs, so that engineering costs associated with analog computer installations might be higher.

In discussing costs, we should be careful to compare like entities. The usual analog computer is not equipped for alarm and logging functions, and any fair cost comparison should include the cost of the equipment for performing these functions as well as the strictly computational part of the control job.

Reliability

Designers of either analog or digital computers face a difficult task in providing the kind of reliability desired by the process industries. One process engineer of my acquaintance has said that 10,000 hours ofuninterrupted service should be the goal; this time amounts to almost 14 months on a 24-hour-a-day basis! Actually, most processing units are shut down at regular or irregular intervals, and scheduled maintenance could be performed much more frequently than once every 14 months.

Reliability is an inverse function of the amount of equipment involved in the system. Small analog computers may therefore offer the most reliable solution for simple control jobs, while digital computers may be preferable to an equivalent assemblage of analog components for large and complicated control jobs.

By attention to details, it should be possible to design either type of computer with the necessary reliability. Both types will be subject to unpredictable complete failures; the analog computer may be more susceptible to unsuspected gradual deterioration which leads to faulty operation but not to complete failure.

Applications

Both analog and digital computers have been or will be used in the following control applications. We do not have access to the reasoning that went into selection of the computer for these applications, but we can describe some features of the systems.

Electric Power Systems

Several utilities are using analog computers to figure continuously the best way to supply electricity to their customers.[2–4] The problem here is to insure that the total load is divided between the available generating stations in such a way that the total cost to the utility is a minimum. This problem is solved by a continuous transfer of load from high-cost stations to low-cost stations until the incremental costs of delivered power are equal. The equipment required includes means for measuring the power output of each station, generating signals which represent the corresponding incremental costs, and making adjustments to bring these costs into agreement.

In this application, the optimizing criterion is relatively simple and well understood. Alarm and recording functions are already handled in other ways. Analog computers appear to be an acceptable choice.

Batch Hydrogenation

At the Case Institute of Technology in Cleveland, research has been conducted on computer control of a batch hydrogenation process.[5] Here infrared and refractive index instruments and an analog computer were used to direct the process in such a manner that the desired product was made in a minimum time.

Solution of differential equations, a natural assignment for an analog computer, played a prominent part in this control program. Nevertheless, in concluding their report, the research workers on this project expressed a desire for several improvements in their equipment including:

1) An algebraic equation solver to process information from the two analysis instruments.
2) Magnetic drum storage for smoothing composition data.
3) A magnetic drum storage and computing system for continuous determination of process parameters.

[2] R. H. Travers, "Automatic economic dispatching and load control—Ohio Edison system," *Trans. AIEE*, vol. 76; January, 1957.

[3] K. N. Burnett, D. W. Halfhill, and B. R. Shepard, "A new automatic dispatching system for electric power systems," *Trans. AIEE*, vol. 75; July, 1956.

[4] E. J. Kompass, "The 'early bird' goes automatic," *Control Eng.*, vol. 3, pp. 77–83; December, 1956.

[5] "Process Automation—Report 1, 1954–1956," Case Institute of Technology, Cleveland, Ohio; September, 1956.

4) A time-program controller for automatic start-up and shut-down operations.

These functions, as well as those already included, could be performed by a general-purpose digital computer designed for process control applications.

Chemical Plants

Early in 1956, Burroughs and du Pont cooperated in an experiment of considerable interest.[6] Measurements taken in a chemical plant at Niagara Falls were converted to pulse form, transmitted by telephone wire to Philadelphia, and processed in a digital computer. Yields and material balance data were sent back to Niagara Falls for use by the plant operators.

Although the computer was not connected for direct control of the process, a number of useful things were learned from this experiment. Two advantages of digital systems were highlighted: the ability of digital data to survive long-distance transmission, and the ability of a digital computer to check the validity of data and computed results.

At a meeting on the subject of computer applications in industrial control, Faulkner of Imperial Chemical Industries, Ltd., of England spoke about the problems that would be involved in controlling an ammonia plant.[7] He quoted a conversation in which the plant manager asks the operator to drop the gas composition to $2\frac{1}{2}$ per cent, starting about 4:30 A.M., in order to prepare for a maintenance job the next day. He then says:

"The shift manager is exercising judgment, that is to say he is guessing on the basis of past experience. The fact is, however, that all the data to enable him to make a precise observation are known. It is too much to expect him to do that sort of job at 2 o'clock in the morning. I know that a small analogue black box could be designed for this purpose, but numbers of black-box slide-rules are not, in my opinion, the way to do the job, because this is only one example of many things of that sort which have to be done. A digital computer would do all these various jobs on demand and many others like them, and no reasonable analogue computer could cope with the mass of information which goes to the making of the material efficiency of an ammonia plant."

Careful reading of his remarks indicates that he is thinking here about a computer to assist the manager and not to exercise direct control. Later, he talks about a chemical process and advocates use of a digital computer for getting maximum yield from a parallel bank of reactors, each of which contains catalyst in a different state of activity.

Petroleum Refining

Esso Standard has announced that an automatic data logger-computer will be installed on a fluid catalytic cracker in a new refinery in Cuba.[8] One-hundred-eleven process variables will be measured, converted to digital form, and logged. Some of these quantities, stored in analog form, will be supplied to a programmed general-purpose analog computer which will sequentially determine the following "operating guides":

1) Carbon burning rate,
2) Catalyst circulation rate,
3) Ratio of catalyst flow to oil flow,
4) Ratio of feed to reactor catalyst holdup,
5) Conversion,
6) Per cent weight of hydrogen in coke,
7) Ratio of coke to total feed,
8) Heat duty of fractionator reflux (top),
9) Heat duty of fractionator reflux (middle),
10) Regenerator superficial velocity,
11) Reactor superficial velocity.

This information will be supplied to the operator for his guidance in running the unit; it is not planned to use these computed quantities for direct control. The computations will be made hourly but can be repeated more frequently on demand.

Since this system is not yet in operation, it is too early to tell whether the proposed combination of operational amplifiers, chopper-stabilized electronic multiplier-divider modules, relays, and stepping switches will perform as well as expected. If it should be decided later to use this equipment for direct control, it may be hoped that the selected quantities turn out to be useful in control, that the available computing speeds will be adequate for control, and that program modifications can be made without extensive equipment changes.

Conclusion

It is noteworthy perhaps that at least one manufacturer of analog computers for engineering use now is providing digital input-output by means of punched tape or an electric typewriter. This development, considered in combination with the fact that any digital control computer must work between analog sensing devices and analog controllers, suggests that the comparison should be one of degree, not kind. We should be asking perhaps, "How much analog and how much digital equipment?" not "Analog *or* digital equipment?" since all control systems will be a combination of both.

Both analog and digital computers will be used for process control, the choice depending on the requirements of the particular job. The digital computer appears well-adapted to the changing computational and logging functions that will be encountered, for example, in large and complicated petroleum or chemical processes. Analog computers have found and will continue to find application in a variety of simpler control problems.

[6] E. W. James, J. Johnson, E. W. Yetter, and M. A. Martin, "How a systems team engineered a plant computer test," *Control Eng.*, vol. 3, pp. 83–86; November, 1956.

[7] I. J. Faulkner, "Introduction to session on the application of digital computers in industrial control," *Proc. IEE*, vol. 103, part B, pp. 98–99; 1956.

[8] "Will the logger-computer optimize refining?" *Control Eng.*, vol. 4, pp. 23–29; March, 1957.

Analysis of a Nonlinear Control System for Stabilizing a Missile*

LEONARD ATRAN†

Summary—**An autopilot with attitude and rate feedback, representative system lags, and a two-way relay servo with inherent hysteresis is considered for roll control of a missile with peripheral, tangentially operating jets.**

This type of control system is shown to produce a steady-state oscillation. Missile dynamics in the presence of this hunting are developed and the relationships governing angular position and rates are found to be functions of the oscillation frequency, control force magnitude, and missile constants (geometry and weight).

The describing function technique is utilized to determine graphically the relationship among frequency, hysteresis band, and system time delays. A comparison is made between the root locus and amplitude-phase presentation. An analog computer study of system behavior is presented to illustrate the agreement between the analysis and system performance.

Introduction

ONE of the foremost considerations in the design of a missile control system is that it be as simple and inexpensive as possible. This can be achieved by using only those components which are absolutely necessary to perform the control task adequately. Gyros, resolvers, amplifiers, filter networks relays, and actuator hardware should be kept to a minimum.

This paper shall restrict itself to the discussion of roll stabilization by means of a relatively simple and reliable autopilot system designed to provide attitude control, whereas the missile maneuver commands in this case are applied to the pitch and yaw channels.

Although in aircraft operation almost any continuous oscillation is intolerable, in an unmanned missile it is possible that a steady-state oscillation confined to reasonable limits is entirely satisfactory. The control system under discussion consists in part of a relay servo driving a jet nozzle valve in such a manner as to produce a continuous dither. The nozzles themselves are located on the periphery of a plane normal to the main thrust line. Control of the jets results in a fixed torque in either of opposite directions.

The autopilot signal required to roll stabilize is derived from an attitude gyro; however, a derivative signal is necessary to augment the negligible aerodynamic damping of the missile.

Missile Roll Dynamics

Let us assume a general missile configuration as shown in Fig. 1.

The roll moment equation, taken about the body axis is:

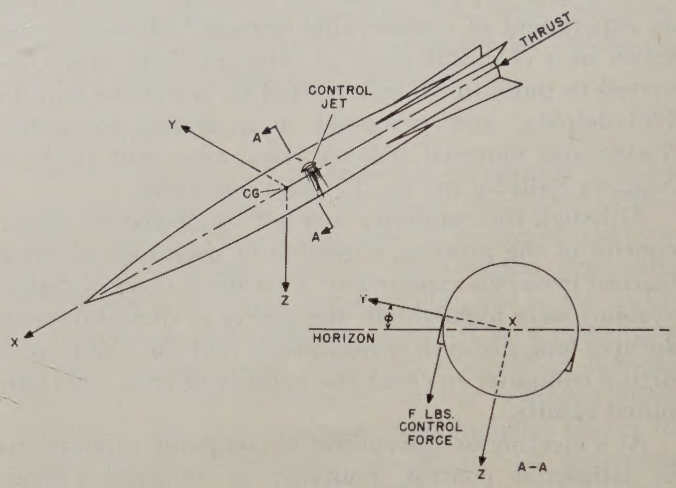

Fig. 1—Missile coordinate system.

$$I_x\dot{P} + (I_z - I_y)QR - I_{xz}(\dot{R} + PQ)$$
$$= \sum L \text{ (summation of roll moments).} \quad (1)$$

Because of symmetry, we may assume

$$I_y = I_z \quad \text{and} \quad I_{xz} = 0.$$

Eq. (1) in simplified form becomes:

$$\dot{P} = l_j f_j + l_m f_m, \quad (2)$$

where

$l_j = L_j/I_x$ (control moment effectiveness),
$l_m = L_m/I_x$ (misalignment torque factor),
f_j = force produced by control jets,
f_m = net unbalanced force due to possible thrust misalignment,
L_j = control force moment arm,
L_m = effective moment arm upon which unbalanced forces act.

With no unbalanced torques acting on the system, $f_m = 0$; therefore, upon integrating (1), we arrive at the following expression for roll rate:

$$P = l_j f_j[t - t \text{ switching}] = \dot{\phi} \text{ (missile roll rate).} \quad (3)$$

During any "on-time"

$$f_j = \pm F \text{ (pounds)} = \text{constant.}$$

The on-time for each unidirectional blast is π/ω where ω is the frequency of oscillation in rad/sec. The peak roll rate is, therefore:

$$\dot{\phi}_{\max} = \frac{-90 l_j F}{\omega} \text{ (deg/sec).} \quad (4)$$

* Manuscript received by the PGAC, September 9, 1956. Presented at WESCON, Los Angeles, Calif., August, 1956.
† Air Arm Div., Westinghouse Electric Corp., Baltimore, Md.

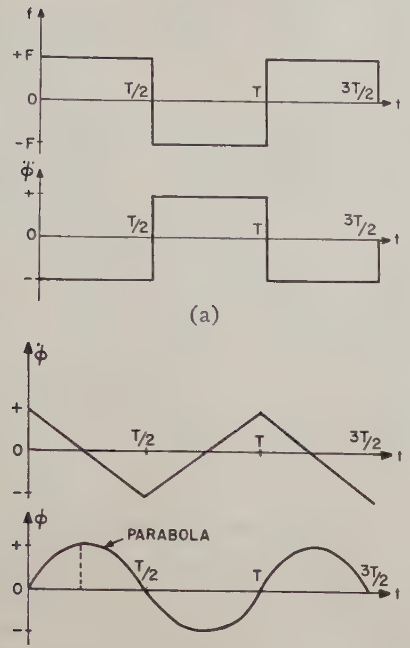

Fig. 2—(a) Waveforms of force and acceleration. (b) Waveforms of roll position and rate.

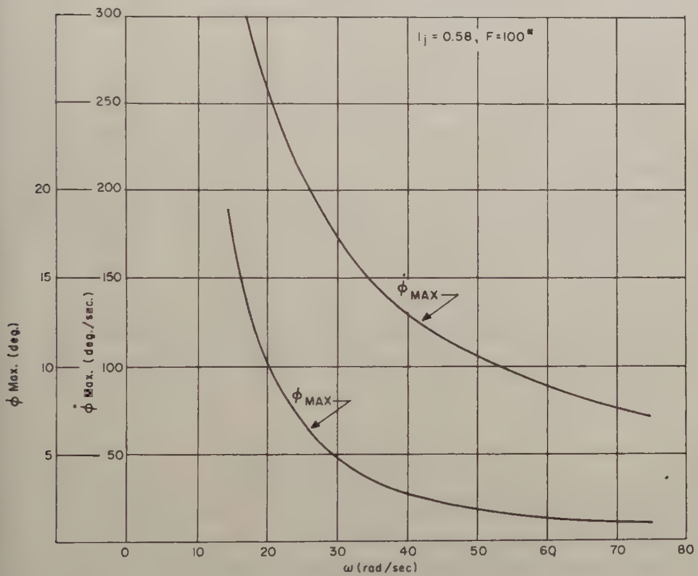

Fig. 3—Plot of maximum roll angle and roll rate vs frequency of acceleration.

Further integration leads to the following expression for the peak roll angle:

$$\phi_{\max} = \frac{-71 l_j F}{\omega^2} \text{ (deg)}. \tag{5}$$

The waveforms of the system under steady-state conditions are illustrated in Fig. 2(a) and 2(b).

Plots of $\phi_{\max}$ and $\dot{\phi}_{\max}$ vs mode frequency are shown in Fig. 3 for values of $l_j = -0.58$ and $F = 100$ pounds.

Superposition of an unbalanced torque requires the development of a counter moment of the same average value, thereby necessitating that the symmetry of the control force vs time curve be destroyed. This is illustrated in the REAC recordings of Fig. 4.

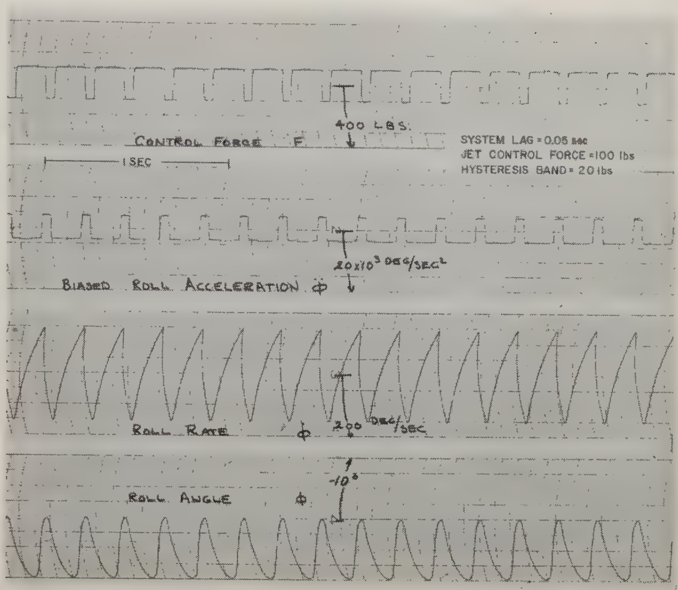

Fig. 4—Relay servo controlling missile in roll (externally applied torque of 49 pounds-feet).

Servosystem

The input-output waveforms of the relay-actuator combination are illustrated in Fig. 5, next page.

The autopilot control system is shown in block diagram form in Fig. 6.

In an effort to determine the behavior of the system in the presence of a highly nonlinear servo, the system transfer functions are combined and the characteristic equation rearranged to the following expression for neutral stability:[1]

$$\frac{-1}{N(x)} = \frac{l_j B(\tau_1 s + 1)}{s^2(\tau_2 s + 1)(\tau_3 s + 1)}, \tag{6}$$

where $\tau_1 = A/B$.

The describing function $N(x)$ has been derived in the Appendix; in addition, both sides of (6) are plotted in Fig. 7. The crossover point of the describing function curve and system transfer function determines both the frequency and amplitude of the resultant steady-state oscillation.

Autopilot Parameters

It has been shown that for the nonlinear system under discussion the magnitude of the roll angle excursions is a function of the control force and the frequency of oscillation. In turn, the frequency is a function of the hysteresis band, system time lags, and autopilot gain. The interrelation will now be explored.

A steady-state torque unbalance, due in part to a misalignment of the thrust axis, will compel the missile to assume a steady-state angular error. However, the system will continue to oscillate in accordance with the

[1] E. C. Johnson, "Sinusoidal analysis of feedback control systems containing nonlinear elements," *Trans. AIEE*, vol. 71, part 2, pp. 169–181; July, 1952.

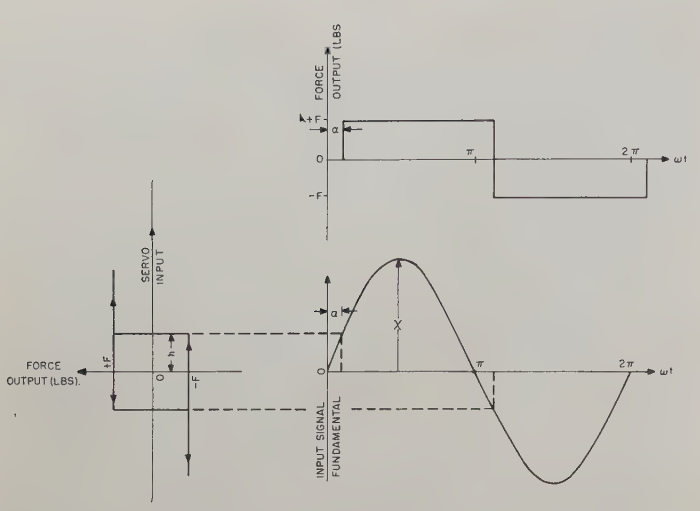

Fig. 5—Control system waveforms.

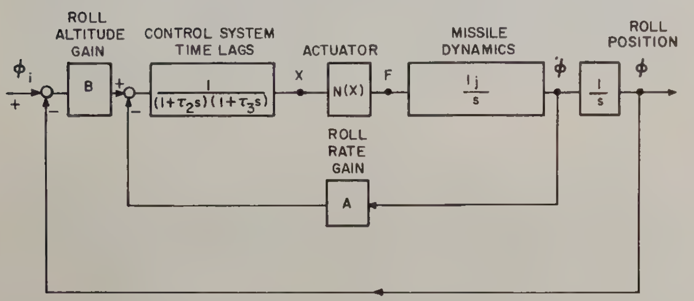

Fig. 6—Control system block diagram.

requirements imposed by (6), and the bias from its original zero steady-state roll angle may be determined in the following manner.

Assume for the moment that the roll oscillation caused by system nonlinearity is sufficiently removed in frequency from the actual roll control mode corner frequency for complete decoupling to exist. That is, the response to a roll command input is not influenced by the higher frequency dither. Under these conditions we may write that

$$\dot{\phi} = 0$$

and average

$$f_{j\text{ave}} = B\phi_{\text{ave}}.$$

Substituting the above into (2) we have:

$$\phi_{\text{ave}} = -\frac{L_m}{L_j B} f_m \text{ (rad).} \tag{7}$$

Thus if the maximum allowable roll angle is specified together with the magnitude of the unbalanced torques likely to be encountered, the required autopilot gain becomes:

$$B = \frac{L_m f_m}{L_j \phi_{AV}} \text{ (pounds/rad).}$$

To counterbalance the moment $L_m f_m$ requires a force capability of

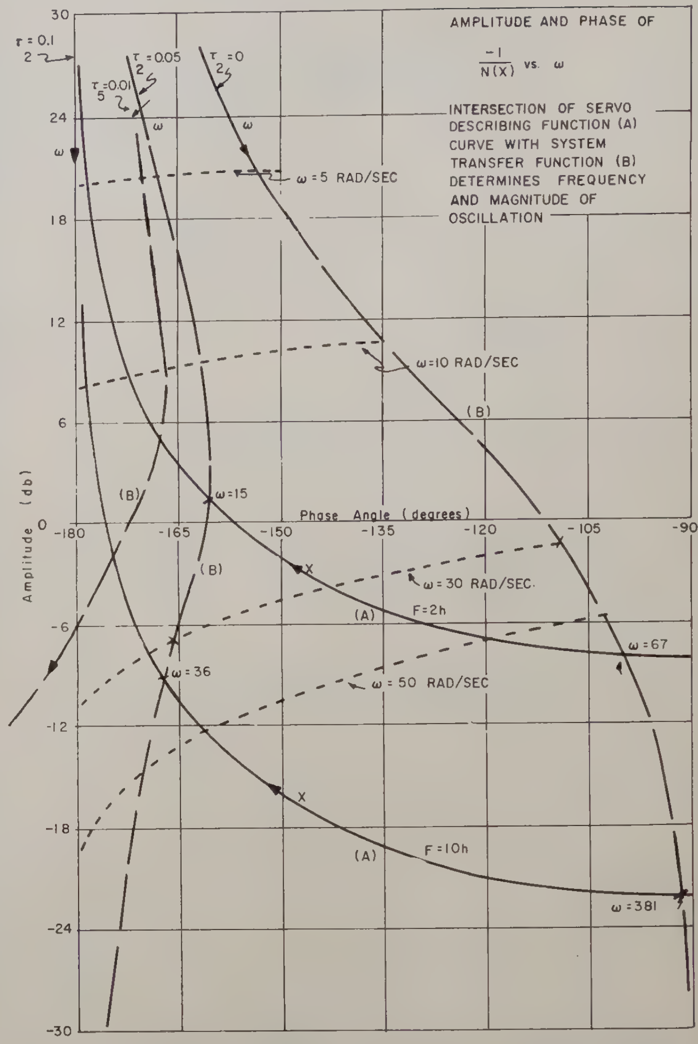

Fig. 7—Amplitude and phase of servo describing function and system transfer function.

$$F = \frac{L_m f_m}{L_j} \text{ (pounds).}$$

The roll mode, regarded as linear and of the form $s^2 - Al_j s - Bl_j = 0$, has a damping factor

$$\zeta_n = \frac{-Al_j}{2\omega_n} \tag{8}$$

where

$$\omega_n = \sqrt{-Bl_j}.$$

Thus for a specified ζ, the value of A that is necessary is

$$A = \frac{2\zeta_n \omega_n}{-l_j}.$$

Discussion

A missile control system was selected for analysis and the following values were assigned to the various parameters.

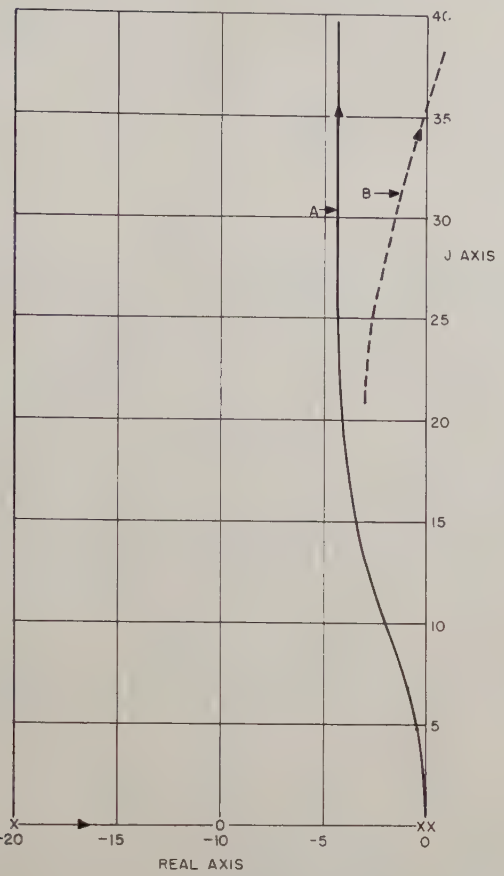

Fig. 8—Root locus plot of representative control system showing effect of nonlinearity. A = linear system, B = nonlinear system. $\tau_2 = 0.05$ sec, $F = 10h$.

$$l_j = -0.58 \frac{1}{\text{pound} - \text{sec}^2},$$

$$F = 100 \text{ pounds},$$

$$A = 42 \text{ pounds/rad/sec},$$

$$B = 420 \text{ pounds/rad},$$

$$\tau_2 = 0, 0.05, 0.1 \text{ second},$$

$$\tau_3 = 0.01 \text{ second for } \tau_2 = 0.05,$$

$$h = 0.1F, 0.5F.$$

Time lags τ_2 and τ_3 were considered as representative delays for this type system.

Autopilot and missile characteristics, as illustrated by Figs. 7–9, result in the following observations.

To limit the amplitude of the roll angle oscillation to $\pm 3.5°$ requires the missile to oscillate at approximately 5.5 cps. Thus an autopilot lag of 0.05 second and a hysteresis/force ratio of 0.1 will satisfy this condition. An increase in either time delay or hysteresis results in a lowering of the natural frequency and a consequent increase in the signal amplitude level, a factor of importance for a system operating close to saturation.

The root locus plot,[2] while providing the requisite stability information, proves to be somewhat more difficult to construct as a result of this particular nonlinearity. The actual procedure consisted of obtaining a family of loci for a series of describing function phase angles, then plotting on each "phase" locus the gain corresponding to the describing function amplitude. To analyze the effects of additional lags demands a complete new family of loci, whereas the amplitude-phase presentation requires but a modified plot of the system transfer function.

A computer (REAC) study resulted in reasonable agreement between the analysis and actual system performance, the frequency and amplitude checking to within 10 per cent thereby justifying the assumption regarding the filtering of higher harmonics.

For example, in Figs. 7 and 8, a resonant point exists at $\omega = 36$ rad/sec when $\tau_2 = 0.05$ sec and $F = 10h$ for the system under discussion. Fig. 9 illustrates the results of a REAC study with agreement as to frequency of oscillation; the theoretical amplitudes may be found in Fig. 3.

[2] W. R. Evans, "Graphical analysis of control systems," *Trans. AIEE*, vol. 67, p. 85; January, 1948.

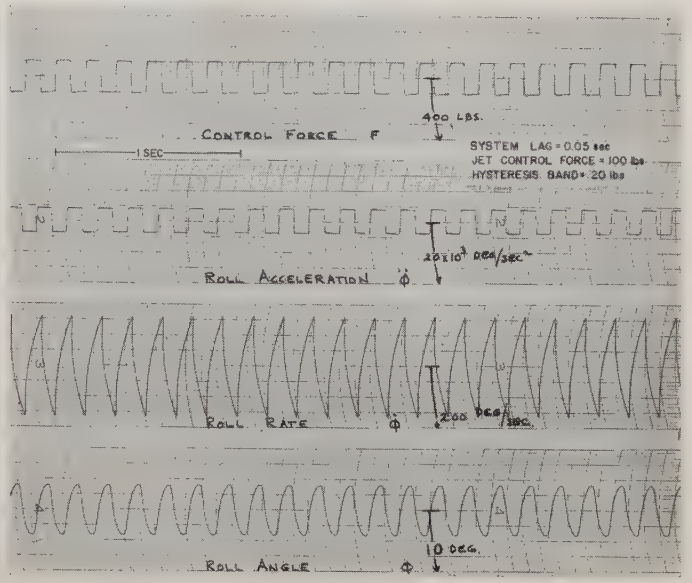

Fig. 9—Relay servo controlling missile in roll.

Conclusion

1) Unbalanced torques should be minimized to reduce the control force.

2) The frequency of the roll oscillation must be maintained at a reasonably high value so as to restrict the magnitude of the roll oscillation and to reduce coupling with the roll control mode.

3) Hysteresis and time lags due to nonideal components must be minimized within the autopilot in order for the system to achieve the necessary resonant frequency.

4) The describing function technique may be readily employed as an analytic tool in the study of a missile autopilot system having a relay servo.

Appendix

Derivation of the Describing Function

Considering the waveform to be a periodic odd function, with the period divided equally, the time function in terms of a Fourier series is

$$f(t) = \sum a_n \sin n(\omega t - \alpha) \tag{9}$$

where

$$a_n = \frac{2}{\pi} \int_0^\pi f(x) \sin nx dx = \frac{2F}{\pi n}(1 - \cos n\pi). \tag{10}$$

From (9) we have that one term of $f(t)$ is:

$$A_n \cos n\omega t + B_n \sin n\omega t$$

where

$$A_n = - a_n \sin n\alpha.$$

$$B_n = a_n \cos n\alpha.$$

Consider initially the effects of harmonics that are of a higher order than the fundamental as being negligible; *i.e.*, $n=1$ only.

Substituting into (10) we find that

$$a_1 = \frac{4F}{\pi},$$

and

$$A_1 = \frac{-4F}{\pi} \sin \alpha$$

$$B_1 = \frac{4F}{\pi} \cos \alpha.$$

However, from Fig. 5,

$$\sin \alpha = \frac{h}{x}$$

and

$$A_1 = \frac{4Fh}{\pi x}$$

$$B_1 = \frac{4F\sqrt{x^2 - h^2}}{\pi x}.$$

The describing function is

$$N(x) = \frac{\sqrt{A_1^2 + B_1^2}}{x} \tag{11}$$

and

$$\frac{-1}{N(x)} = \frac{x}{\sqrt{A_1^2 + B_1^2}} \underline{/\pi - \beta} \tag{12}$$

where

$$\beta = \tan^{-1} B_1/A_1.$$

Upon substituting for A_1 and B_1, we arrive at the required relationship that

$$\frac{-1}{N(x)} = \frac{\pi}{4}\left(\frac{x}{F}\right), \quad \underline{/-180° + \sin^{-1} h/x.} \tag{13}$$

Glossary

Roman Symbols

A = roll rate gain (pounds/rad/sec).
A_1, A_n = Fourier coefficients.
a_1, a_n = Fourier coefficients.
B = roll attitude gain (pounds/rad).
F, f = control force (pounds).
h = hysteresis (pounds).
I_x, I_y, I_z, I_{xz} = moments and product of inertia (slug $-$feet^2).
j = jet control subscript, also $\sqrt{-1}$.
L = roll moment (pound$-$feet).
$N(x)$ = servodescribing function.
n = integer of harmonic.
P = roll rate (rad/sec).
Q = pitch rate (rad/sec).
R = yaw rate (rad/sec).
s = Laplace operator.
t = real time (sec).
X = amplitude of servoinput signal, roll axis of missile.
Y = missile pitch axis.
Z = missile yaw axis.

Greek Symbols

α = phase lag.
β = phase angle (deg).
τ = system time delay (sec).
ϕ = roll angle (rad).
ω = radian frequency (rad/sec)
ζ = damping factor (nondimensional).

Acknowledgment

The author wishes to acknowledge the encouragement and advice provided by A. M. Fuchs now of CDC Control Services, Inc.

Root Locus Method of Pulse Transfer Function for Sampled-Data Control Systems*

MASAHIRO MORI†

Summary—The pulse transfer function is a powerful tool for analysis and synthesis of sampled-data systems. The author has extended the root-locus method[1] to the region of the pulse transfer function so that we can analyze and synthesize the sampled-data systems by the analogous method for the continuous-data systems.

The results are as follows: the rules by which the root loci of the pulse transfer function can be plotted are identical to those of the continuous-data systems. The conditions for absolute and relative stabilities for the sampled-data systems on the z plane are conformal to those for the continuous-data systems on the s plane.

Existence of a finite settling time in a sampled-data control system has been pointed out by the root-locus method.

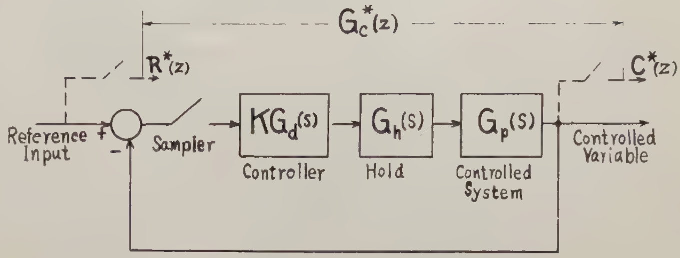

Fig. 1—Typical sampled-data control system.

Introduction

GENERALLY, the pulse transfer function (ptf)[2,3] G^* is a rational function of e^{sT} and can be written

$$G^*(e^{sT}) = \frac{N^*(e^{sT})}{D^*(e^{sT})} = \frac{N^*(z)}{D^*(z)} = G^*(z) \tag{1}$$

where $z=e^{sT}$, T is the sampling period, and N^*, D^* denote polynomials in z. The order of z in the denominator D^* is equal or higher than that of the numerator N^*. G^* is a function of s, hence, of z. Therefore, the root locus may be defined on the s plane as well as on the z plane. But, since G^* is a rational function of z and a transcendental function of s, it is more expedient to define root loci in the z plane than on the s plane.

The root loci of pulse transfer functions are defined as plots of the variations of the poles of the closed-loop pulse transfer functions on the z plane with changes in the open-loop gain. In this paper, the root loci are termed "z loci," and correspondingly, the root loci on the s plane for the continuous-data systems are termed as "s loci."

With reference to Fig. 1, the closed-loop ptf $G_c^*(z)$ is given as

$$G_c^*(z) = \frac{C^*(z)}{R^*(z)} = \frac{KG^*(z)}{1+KG^*(z)} \tag{2}$$

where $G^*(z)$ is the open-loop ptf, that is, $G^*(z)$ is the z transform of impulsive response of the system whose transfer function is $G_d(s)G_h(s)G_p(s)$. K is the open-loop gain.

Accordingly, the z locus for the system shown in Fig. 1 is the locus of the root of the following characteristic equation as K is varied from zero to infinity.

$$1 + KG^*(z) = 0. \tag{3}$$

Rules for Construction of z Loci

As mentioned above, the continuous system transfer function is the rational function of s, and the ptf is the rational function of z. Accordingly, the rules of the s loci which are based upon the rational form must be applicable to the z loci. Such rules are as follows:

1) For a gain $K=0$ the roots of (3) coincide with the poles of $G^*(z)$, and for a gain $K=\infty$ the roots coincide with the zeros of $G^*(z)$. Thus, the z loci start from the poles and arrive at the zeros.

2) The z loci are always symmetrical about the real axis.

3) Phase condition: From (3),

$$KG^*(z) = -1.$$

Hence, with reference to Fig. 2, the phase condition is given as

$$\sum \beta - \sum \alpha = -180° \pm 360° \times n \tag{4}$$

where β is the angle of the vector from a zero of $G^*(z)$ to the root Q, and α is the angle from a pole of $G^*(z)$ to Q as shown in Fig. 2, and n is an integer.

4) Asymptotes: If the number of poles n exceeds the number of zeros m, there are $n-m$ branches which terminate at the zeros located at infinity. The directions of the infinite asymptotes of the z loci are shown in Table I. All asymptotes intersect at a point ρ_a on the real axis, where

$$\rho_a = \frac{\sum_{i=1}^{n} p_i - \sum_{i=1}^{m} z_i}{n-m}$$

* Manuscript received by the PGAC, January 1, 1956. Presented at the Symposium of The Society of Automatic Control in Japan, June 29, 1954. Published in *Automatic Control (Japan)*, vol. 2, pp. 5–12; March 1, 1955.

† Univ. of Tokyo, Yayoichō, Chiba City, Japan.

[1] W. R. Evans, "Graphical analysis of control systems," *Trans. AIEE*, vol 67, pp. 547–551; 1948.

[2] F. Hurewicz, "Theory of Servomechanisms, H. M. James, N. B. Nichols, and R. S. Phillips," M.I.T. Rad. Lab. Ser., McGraw-Hill Book Co., Inc., New York, N. Y. vol. 25, ch. 5; 1947.

[3] R. H. Barker, "The pulse transfer function and its application to sampling servo systems," *Proc. IEE*, part 4, monograph no. 43, pp. 302–317; July, 1952.

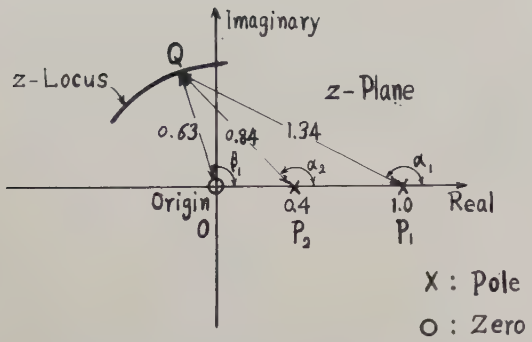

Fig. 2—Illustration for gain and phase conditions.

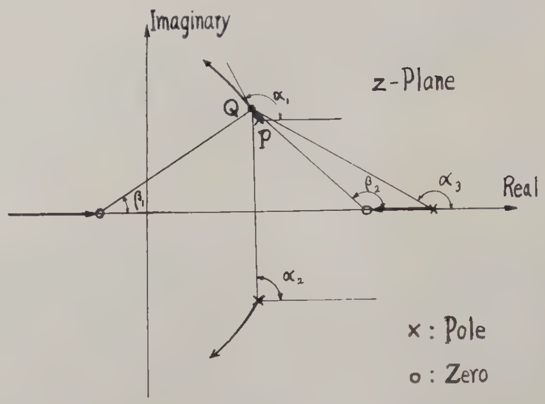

Fig. 3—Evaluation of angle departure.

TABLE I
DIRECTIONS OF ASYMPTOTES

n-m	Directions			
1	180°			
2	−90°	+90°		
3	−60°	+60°	+180°	
4	−45°	+45°	−135°	+135°

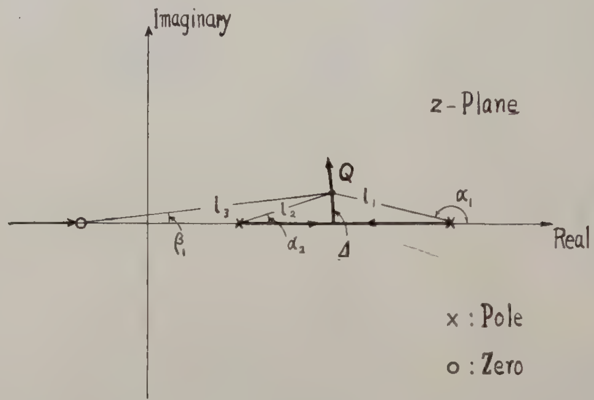

Fig. 4—Determination of intersection with the real axis.

provided p_i = pole and z_i = zero.

5) Angles of departure and arrival: The angles at which the z loci leave the poles and arrive at the zeros can be evaluated from (4). For example, in Fig. 3 we wish to determine the angle departure of the z locus from pole P. Let us consider a point Q on the z locus a small distance away from the pole P. This point Q must be at an angle α_1 from P such that,

$$(\beta_1 + \beta_2) - (\alpha_1 + \alpha_2 + \alpha_3) = -180° \pm 360° \times n.$$

6) The z locus exists on a part of the real axis where an odd number of poles plus zeros are found to the right. This may be verified easily by (3).

7) Intersection with the real axis: If the displacement from the real axis is Δ and this is intentionally made very small, then in Fig. 4,

$$180° - \alpha_1 = \Delta/l_1$$
$$\alpha_2 = \Delta/l_2$$
$$\beta_1 = \Delta/l_3.$$

Applying the condition to rule 3),

$$\beta_1 - \alpha_2 - \alpha_1 = -180°$$
$$\Delta/l_3 - \Delta/l_2 = -\Delta/l_1.$$

Thus,

$$1/l_2 - 1/l_3 = 1/l_1. \tag{5}$$

Thus the intersection may be determined as a point where the equality indicated in (5) exists.

8) Gain condition: From (3),

$$K = \frac{1}{|G^*(z)|}.$$

A graphical procedure is convenient to evaluate values of K along the z loci by this relation. For example, if $G^*(z) = 0.6z/(z-1)(z-0.4)$, with reference to Fig. 2,

$$K = \left|\frac{(z-1)(z-0.4)}{0.6z}\right| = \frac{P_1Q \times P_2Q}{0.6 \times 0Q}$$
$$= \frac{1.34 \times 0.84}{0.6 \times 0.63} = 3.0$$

Thus, gain K can be evaluated in terms of the vectors from the poles and zeros to the point on the z locus.

9) Centroid of the roots: As mentioned by Yeh,[4] the centroid ρ of the roots, which is given by

$$\rho = \frac{1}{n} \sum_{i=1}^{n} p_i$$

is an invariant of the system if $n - m \geqq 2$; it will shift by an amount equal to K/n if $n - m = 1$.

10) Loci of simple ptf: The ptf having n poles and m zeros shall be referred to as type (n, m). Loci of type $(n \leqq 2, m \leqq 2)$ are straight lines or circles as shown in Table II.[4]

[4] V. C. M. Yeh, "The study of transients in linear feedback system by conformal mapping and root-locus method," *Trans. ASME*, vol. 76, pp. 349–361; 1954.

TABLE II

Z LOCI OF SIMPLE PULSE TRANSFER FUNCTIONS

Type	Shape	
(1, 0)	Straight line from the pole to minus infinity on real axis	
(1, 1)	Straight line between the pole and the zero on real axis	For type (2, 1) and type (2, 2), $\begin{cases} \text{pole} = \mu_1 + j\nu,\ \mu_2 - j\nu \\ \text{Zero} = \xi_1 + j\eta,\ \xi_2 - j\eta \\ \text{Radius} = r \end{cases}$ ↓
(2, 0)	For two real roots: Segment between the two poles and perpendicular bisector of the segment For conjugate complex roots: Straight line through the two roots (except segment between the roots)	
(2, 1)	Circle (its center is on real axis)	Center $= \xi_1$ $r^2 = (\mu_1 - \xi_1)(\mu_2 - \xi_2) + \nu^2$
(2, 2)	Circle	Center, $0 = \dfrac{(\mu_1\mu_2 + \nu^2) - (\xi_1\xi_2 + \eta^2)}{(\mu_1 + \mu_2) - (\xi_1 + \xi_2)}$ $r^2 = 0^2 + \dfrac{(\mu_1 + \mu_2)(\mu_1\mu_2 + \nu^2) - (\xi_1 + \xi_2)(\xi_1\xi_2 + \eta^2)}{(\mu_1 + \mu_2) - (\xi_1 + \xi_2)}$

STABILITY CRITERION

Generally speaking, if all singular points of the ptf are located inside the unit circle, the sampled-data system is said to be stable with regard to output values only at sampling instants. If at least one singular point lies outside the unit circle, the system is unstable.

The system is stable if all roots of (3) are located inside the circle. This constitutes the necessary and sufficient condition of the closed-loop system stability.

The unit circle in the z plane corresponds to the imaginary axis of the s plane.

TRANSIENT RESPONSE

Relation Between the Location of the Root and the Shape of the Indicial Response

Information on the effects of the roots on the transient responses are given by inverse z transformations. When the reference input is the unit step, the output sequence c_k is given by:

$$c_k = Z^{-1}\left[G_c^*(z) \frac{z}{z-1} \right] \tag{6}$$

where Z^{-1} denotes the inverse z transformation.[5] Thus, in general,

$$c_k = \frac{1}{2\pi j} \oint \frac{K \prod_{i=1}^{d} (z - z_i) \prod_{i=1}^{f} \{(z - \xi_i)^2 + \eta_i^2\}}{\prod_{i=1}^{g} (z - r_i) \prod_{1=i}^{h} \{(z - \mu_i)^2 + \nu_i^2\}}$$

$$\frac{z}{(z-1)} z^{k-1} dz \tag{7}$$

where the path of integration in (7) is a closed contour enclosing all the singular points of $G_c^*(z)$ and r_i = real root of (3), $\mu_i \pm j\nu_i$ = conjugate complex roots of (3), z_i = real zero of (2), $\xi_i \pm j\eta_i$ = conjugate complex zeros of (2), and $g + 2h \geqq d + 2f$.

Evaluating the contour integral, we obtain

$$c_k = \sum_i \left| R_i \right| r_i^k + \sum_i 2 \left| I_i \right| (\mu_i^2 + \nu_i^2)^{k/2} \cos(k\theta_i + \phi_i) \tag{8}$$

where R_i is residue of the real root r_i, I_i is residue of the complex root $\mu_i + j\nu_i$, θ_i is phase of the complex root $\mu_i + j\nu_i$, and ϕ_i is phase of the residue I_i.

In the following discussions, it is assumed that all roots have absolute values less than unity. In (8), if r_i is positive, r_i^k decreases uniformly as k increases, and converges to zero. If r_i is negative, r_i^k is oscillatory and converges to zero. Hence, a positive real root represents a uniform variation and a negative real root represents a damped oscillation.

Now, let us focus attention on the second term. It is apparent from previous assumptions that the absolute value of a pair of conjugate complex roots, *i.e.*, $(\mu_i^2 + \nu_i^2)^{1/2}$ is less than unity. Therefore, each component of the second term which comes from a pair of conjugate complex roots describes a damped oscillation.

Consequently, it can be concluded that a uniform variation comes from a positive real root and a damped oscillation is from a negative real root or from a pair of conjugate complex roots.

Also, it is clear from above that the intersection of the z locus with the positive real axis indicates critical damping.

In addition to these results, it is noted that output at the steady state comes from a real root at the point of (+1, 0). This can be deduced from the first term of (8) or from the final value theorem for z transforms.[6]

These relations are conformal to those at the continuous-data systems in the s plane, and are arranged in Table III.

[5] C. H. Smith, D. F. Lawden, and A. E. Bailey, "Characteristics of Sampling Servo Systems," in A. Tustin, "Automatic and Manual Control," Butterworths Scientific Publications, London, Eng.; 1952.

[6] J. R. Ragazzini and L. A. Zadeh, "The analysis of sampled-data systems," *Trans. AIEE*, vol. 71, part 2, pp. 225–232; 1952.

TABLE III

CONFORMAL RELATIONSHIP BETWEEN THE s PLANE AND THE z PLANE

	s plane	z plane
	Origin	$(+1, j\cdot 0)$
	Real axis	Positive real axis
	Imaginary axis	Unit circle
	Right half plane (width is $2\pi/T$)	Outside of the unit circle
	Left half plane (width is $2\pi/T$)	Inside of the unit circle
Stability criterion	Left half plane	Inside of the unit circle
One uniform variation	One negative real root	One positive real root
One damped oscillation	One pair of conjugate complex roots	One negative real root or one pair of conjugate complex roots
Critical damping	Intersection of s locus with negative real axis	Intersection of z locus with positive real axis
Output at steady state	Root at the origin	Root at point $(+1, j\cdot 0)$
Constant $-\zeta$ curve	Straight lines l, l' in Fig. 5 (a)	Heart-shaped curve in Fig. 5 (b)

Constant-ζ Curve

Now the damped oscillation discussed above will be studied more quantitatively in the following.

An output sequence from a component of the second term of (8) is,

$$c_k = 2\left| I_i \right| \left| q_i \right|^k \cos (k\theta_i + \phi_i), \tag{9}$$

where $q_i = \mu_i + j\nu_i$, and $|q_i| = (\mu_i^2 + \nu_i^2)^{1/2}$.

If one assumes a continuous output wave of damped cosine form, c_k being the sampled values, one can apply the concept of damping, and define the following amplitude ratio:

$$r_d = \frac{(c_k)_{k=2\pi/\theta_i}}{(c_k)_{k=0}}. \tag{10}$$

The relation between r_d and the complex root q_i is obtained by substituting (9) in (10) as follows:

$$r_d = \frac{2\left| I_i \right| \left| q_i \right|^{2\pi/\theta_i} \cos (2\pi + \phi_i)}{2\left| I_i \right| \left| q_i \right|^0 \cos \phi_i} = \left| q_i \right|^{2\pi/\theta_i}. \tag{11}$$

Hence, the condition for an output with amplitude ratio r_d is:

$$\left(\begin{array}{l} |q_i| = r_d^{\theta_i/2\pi} \\ \angle q_i = \theta_i \end{array}\right. . \tag{12}$$

The locus of (12) is a logarithmic spiral as is shown in Table IV and Fig. 5(b).

On the other hand, the same damping condition for the continuous-data system on the s plane is a line l in Fig. 5(a). Its equation is

$$e^{2\pi\sigma/\omega} = r_d, \tag{13}$$

where $s = \sigma + j\omega$.

TABLE IV

ABSOLUTE VALUE $|g_i|$ AND PHASE θ_i FOR $\zeta = 0.2$ $(r = 0.25)$

Phase θ_i	Absolute value $\|q_i\|$	Phase θ_i	Absolute value $\|q_i\|$
0	1.00	$5\pi/8$	0.65
$\pi/8$	0.92	$3\pi/4$	0.59
$\pi/4$	0.84	$7\pi/8$	0.55
$3\pi/8$	0.77	π	0.50
$\pi/2$	0.71		

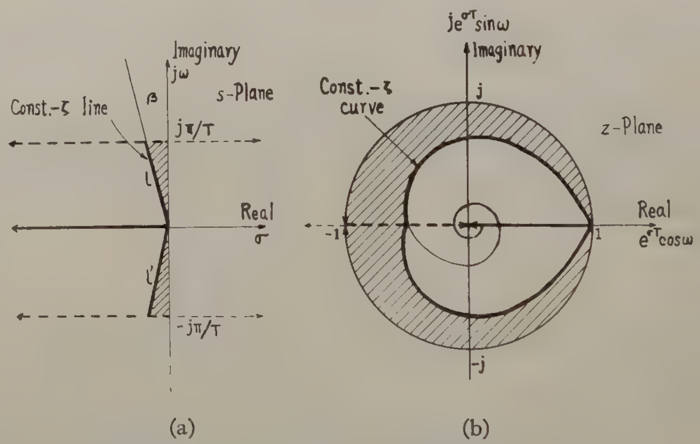

Fig. 5—Conformal relationship between the s plane and z plane.

Therefore,

$$\sigma/\omega = \frac{1}{2\pi} \log r_d. \tag{14}$$

Transforming this line on the z plane, we get

$$e^{sT} = e^{\sigma T} e^{j\omega T} = r_d^{\omega T/2\pi} e^{j\omega T},$$

which has the following complex value:

$$\left(\begin{array}{l} \text{absolute value} = e^{\sigma T} = r_d^{\omega T/2\pi} \\ \text{phase} = \omega T. \end{array}\right. \tag{15}$$

Comparing (12) with (15), one can see that the spiral in Fig. 5(b) is conformal to the straight line l in Fig. 5(a). Thus, the constant amplitude ratio curve for the sampled-data systems coincides with the transform of that for the continuous-data systems. Also, it is deduced that ω, the imaginary part of s, is angular frequency of the output cosine wave.

The above discussions based upon r_d can be modified in the following statements in terms of conventional damping ratio ζ. Using the angle β shown in Fig. 5(a), ζ can be written as:

$$\zeta = \sin \beta. \tag{16}$$

Referring to (14), we have

$$\tan \beta = \frac{\sigma}{\omega} = \frac{1}{2\pi} \log r_d. \tag{17}$$

Thus,

$$\zeta = \sin \left\{ \tan^{-1} \left(\frac{1}{2\pi} \log r_d \right) \right\}. \tag{18}$$

Therefore, (12) can be rewritten as

$$\begin{cases} |q_i| = e^{(\zeta/\sqrt{1-\zeta^2})\theta_i} \\ \angle q_i = \theta_i. \end{cases} \tag{19}$$

Though $G_c^*(e^{sT})$ contains poles of infinite number, periodic on the s plane, this is equivalent to $G_c^*(z)$ which is characterized by a finite number of poles on the z plane. By the conformal relationship of s and z (see Fig. 5), the inversion integral (7) is specified uniquely by choosing a contour about one periodic strip on the s plane. Consequently, it is obviously justifiable to choose this contour about the first strip bounded by the lines $\pm j\pi/T$. Therefore, though the logarithmic spiral continues infinitely towards the origin as θ_i increases, it should be limited to the part of $\theta_i \leqq \pi$.

Thus, the heart-shaped curve in Fig. 5(b) is the condition for constant ζ. If the conjugate roots are located inside the heart-shaped curve the damping is stronger than that of this condition, and if the roots are located outside, the damping is weaker. Table IV shows polar coordinate of the constant-ζ curve for $\zeta = 0.2$ (or $r_d = 1/4$).

The heart-shaped constant-ζ curve has an intersection with negative real axis for $\theta_i = \pi$. Thus there exists a negative real root which gives a damped oscillation of the specified ζ value. This fact is not surprising because a negative real root inside the unit circle causes a damped oscillation as mentioned before.

Relations Between z Locus and s Locus

It should be noted that the root loci on the z plane, of sampled-data systems, $1+G^*(z)=0$, are not the conformal transformations of root loci of $1+G(s)=0$ on the s plane.

As pointed out by Ragazzini and Zadeh,[6] the following relation was discovered by Poisson.

$$G^*(z) = \frac{1}{T} \sum_{n=-\infty}^{\infty} G(s + 2n\pi j/T), \tag{20}$$

where n is an integer.

Therefore, the z locus of (3) is conformal to root locus on the s plane given by the following:

$$1 + \frac{1}{T} \sum_{n=-\infty}^{\infty} G(s + 2n\pi j/T) = 0. \tag{21}$$

However, plotting this root locus on the s plane is difficult.

Dead Time

Handling a dead time, L, by the s locus of a continuous-data system[7] is not simple, because its transfer function has term e^{-sL} in the numerator.

On the contrary, the z locus of a sampled-data system with a dead time can be plotted as easily as the system with no dead time (see Fig. 6), because the ptf $G_L^*(z)$ which has a dead time L is a rational function of z as follows:

1) When $L = nT$,

$$G_L^*(z) = G^*(z)/z^n \tag{22}$$

where $G^*(z)$ is ptf of the system having no dead time, and n is positive integer.

2) When $L = \delta T$,

$$G_L^*(z) = z^{-1} \sum_{k=0}^{\infty} g_{kT+mT} z^{-k} \tag{23}$$

where g_{kT} is weighting sequence of the system whose ptf is $G^*(z)$, and $0 \leqq \delta < 1$ and $m = 1 - \delta$.

Finite Settling Time

It is evident that in the continuous-data control any linear system has an infinite settling time (time to reach zero error after applying a step input).

On the contrary in the sampled-data control, when the z locus passes through the origin [see the right sides of Fig. 6(a) and (b)], it is possible to cause the system to have a finite settling time[8] so far as the controlled variable at the sampling instants is concerned. If the gain is equal to the value of K at the origin, the impulsive response derived from the zero root becomes a finite polynomial in z^{-1}. This will be demonstrated in example 2).

[7] A. Nomoto, "Contribution of the root-locus analysis of the feedback control system," *Proc. Second Japan Natl. Congress for Appl. Mech.*, pp. 359–362; 1952.

[8] R. C. Oldenbourg, "Deviation Dependent Step-by-Step Control as Means to Achieve Optimum Control for Plant with Large Distance-Velocity Lag," in A. Tustin, "Automatic and Manual Control," Butterworths Scientific Publications, London, Eng.; 1952.

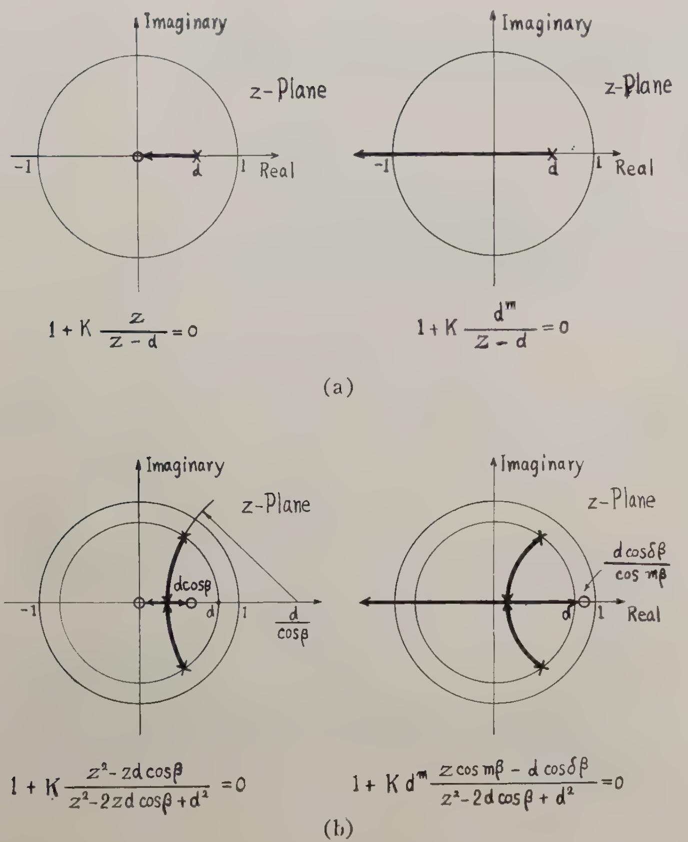

(a) $G(s) = \dfrac{1}{(s+\alpha)}$ (b) $G(s) = \dfrac{s+\alpha}{(s+\alpha)^2+\beta^2}$

Left sides: without dead time, characteristic equation is: $1+KG^*(z)=0$,
Right sides: with dead time less than T, characteristic equation is: $1+KG^*_L(z)=0$.
[See (23).]

Fig. 6—Examples of z locus.

Illustrative Examples

Example 1): In the first example, the gain adjustment of the system shown in Fig. 7 is considered. It is assumed that the specification for damping is $\zeta=0.2$, the continuous transfer function of the controlled system is $e^{-sL}/(s\tau+1)$ and the time constant τ is 60 seconds, the dead time L is 10 seconds. It is postulated also that the sampling period T is 15 seconds and the order of the hold circuit is zero, that is, its transfer function is $(1-e^{-sT})/s$. (See Fig. 8.)

The characteristic equation is written as

$$1+K\left\{\frac{1}{z}-\frac{(z-1)e^{-T/3\tau}}{(z-e^{-T/\tau})z}\right\}=0. \tag{24}$$

Hence,

$$1+K\frac{0.08(z+1.75)}{z(z-0.78)}=0. \tag{25}$$

The z loci can be drawn on the basis of the rules from 1) to 10) as follows: the zero is $(-1.75, 0)$, and the poles are the origin and $(+0.78, 0)$. Therefore, from rule 1)

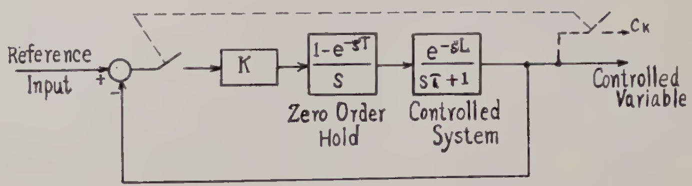

Fig. 7—Sampled-data control system used in illustrative example 1).

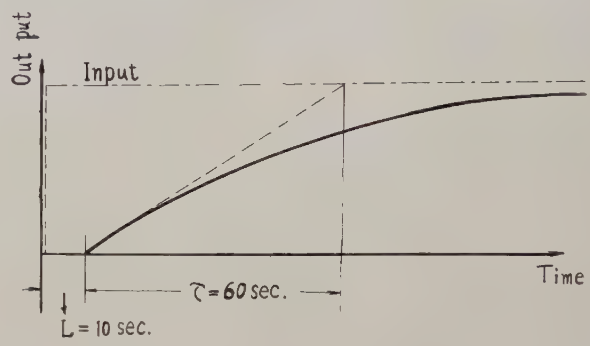

Fig. 8—Indicial response of the controlled system used in illustrative example 1).

the loci start from the origin and $(+0.78, 0)$ and one of the loci terminates at $(-1.75, 0)$. From rules 2) and 4), another locus terminates at minus infinity. From rule 6), the parts of the real axis between the origin and $(+0.78, 0)$, and between minus infinity and $(-1.75, 0)$ constitute sections of the loci. With reference to Table II, since the type of this ptf is (2, 1), the other part of the loci is a circle with a radius 2.11, and the center at $(-1.75, 0)$. Thus the z locus can be drawn easily as shown in Fig. 9.

Constant-ζ curve for $\zeta=0.2$ can be obtained by plotting the complex value q_i of (19).

Then the gain K for $\zeta=0.2$ is determined by finding the value at the intersection of the z locus with the constant-ζ curve. Absolute values of three vectors are required for the evaluation, and by rule 8).

$$K=\left|\frac{z(z-0.78)}{0.08(z-1.75)}\right|=\frac{0.76\times0.90}{0.08\times2.11}=4.0.$$

Under this condition, the indicial response for the reference input may be obtained by (7). [For this purpose, it is more convenient to expand the integrand of (7) into a power series in z^{-1}. The coefficient of the term of z^{-k} is equal to the value of the output at the kth sampling instant c_k].[9]

$$c_k = -2\times0.33\times0.76^{k-1} \times\cos\left\{(k-1)71.5^\circ+45^\circ\right\}+0.80. \tag{26}$$

Fig. 10 shows this response.

Example 2): Here a compensation of a sampled-data control system is demonstrated. The ptf of the system

[9] J. R. Ragazzini and A. R. Bergen, "A mathematical technique for the analysis of linear systems," Proc. IRE, vol. 42, pp. 1645–1651; November, 1954.

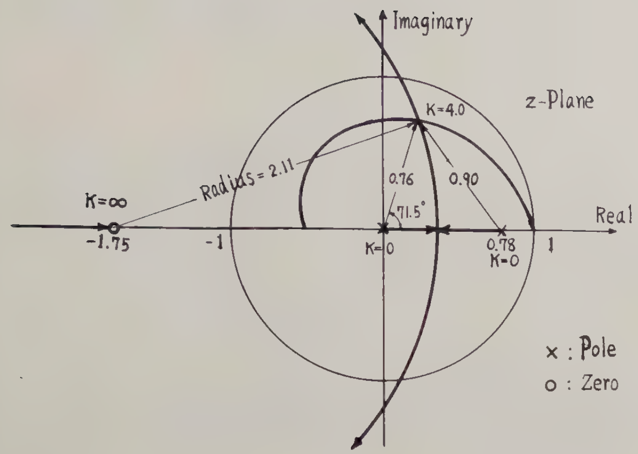

Fig. 9—Z locus of the sampled-data control systems used in illustrative example 1).

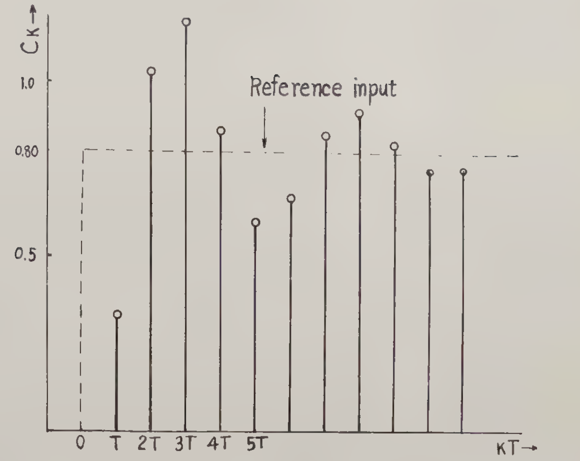

Fig. 10—Indicial response of the sampled-data control system used in illustrative example 1), when gain, K, is 4.0.

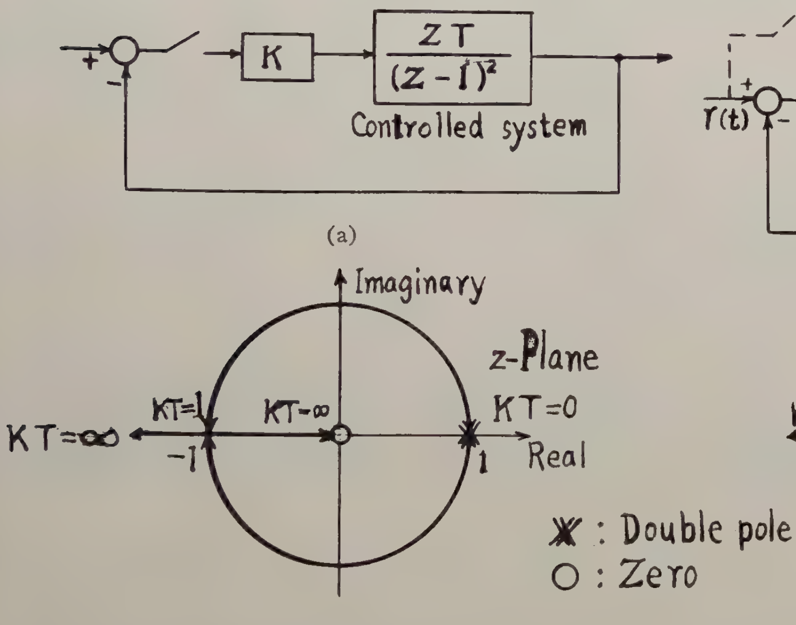

Fig. 11—(a) Sampled-data control system used in illustrative example 2), without compensation. (b) Its z locus

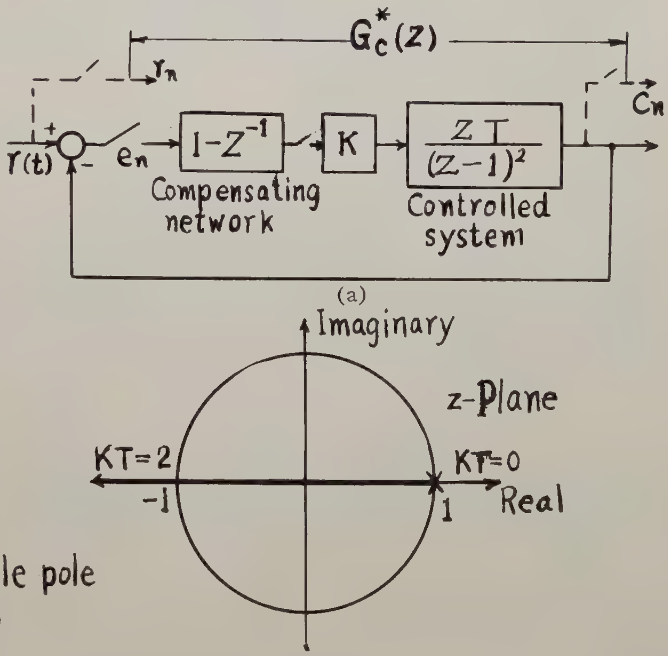

Fig. 12—(a) Sampled-data control system used in illustrative example 2), with compensating network. (b) Its z locus.

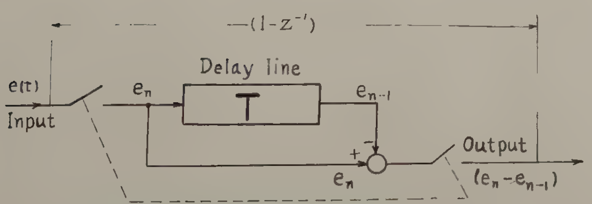

Fig. 13—Compensating pulsed network used in illustrative example 2); e_n is sampled value of input waveform $e(t)$ at time nT.

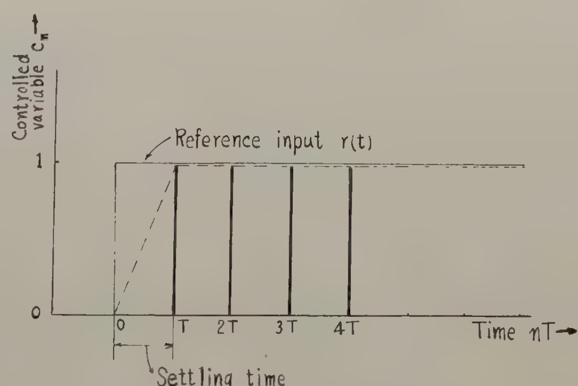

Fig. 14—Indicial response for unit step reference input of the system shown in Fig. 11, (a) $KT=1.0$.

which has the continuous transfer function $1/s^2$ is,

$$G^*(z) = zT/(z-1)^2 \tag{27}$$

where T is the sampling period.

If we construct a sampled-data feedback system simply as shown in Fig. 11 (a), without any compensation[10] the characteristic equation will be,

$$1 + K\frac{zT}{(z-1)^2} = 0. \tag{28}$$

Fig. 11(b) shows this z locus. According to the stability criterion, this system is not stable for any value of KT.

The system may be stabilized by adding a compensating unit in series with the controlled system. The compensating unit is a pulsed network as shown in Fig. 13, and its output at time nT is the difference of two sample values of input at nT and $(n-1)T$,[11] where n is an integer. Then the ptf of this network is $1-z^{-1}$. Thus, the characteristic equation becomes

$$1 + K\frac{T}{(z-1)} = 0. \tag{29}$$

Fig. 12 shows the compensated feedback system and its z locus. The system becomes stable for $0<KT<2$.

If K has the value at the origin, the system has the finite settling time. That is, for this value of K the closed-loop ptf is,

$$G_c^*(z) = \left.\frac{\dfrac{KT}{(z-1)}}{1+\dfrac{KT}{(z-1)}}\right|_{KT=1} = z^{-1}. \tag{30}$$

Fig. 14 shows the control action under this condition. The settling time is only one sampling period and the system has no overshoot.[12]

Discussion

In short, the rules for graphical construction of z loci are equivalent to those for s loci.

Absolute and relative stabilities can be deduced from conformal mapping conditions between s and z. The s plane may be transformed to the z plane in many folds. However, the pertaining region of the s plane should be limited to the strip $\pm j\pi/T$.

When the z locus passes through the origin, it is possible to cause the sampled-data system to have a finite settling time.

The author would like to emphasize the usefulness of the root-locus method not only in continuous-data systems but also in sampled-data systems.

Acknowledgment

The author is sincerely grateful to Prof. Y. Takahashi for his kindness and effort in guiding this research. Thanks are expressed also to Prof. A. Nomoto, Assistant Prof. K. Izawa, and T. Mitsumaki.

[10] In this case, the input to the controlled system is an impulse since the system has no hold circuit.

[11] W. K. Linvill and J. M. Salzer, "Analysis of control systems involving digital computers," Proc. IRE, vol. 41, pp. 901–906; July, 1953.

[12] The z transform method has the limitation of yielding information only at the sampling instants. Therefore, the concept of the finite settling time should be limited only to the controlled variable at the sampling instants. But, as a matter of fact, the system in this example has a finite settling time T in a continuous sense. That is, after the time T, the error of the system becomes zero not only at the sampling instants but also everywhere as shown by dotted line in Fig. 14.

Input-Output Analysis of Multirate Feedback Systems*

GEORGE M. KRANC†

Summary—**A general analytical technique described in this paper permits the extension of Z-transform methods to sampled-data systems containing synchronized switches which do not operate with the same sampling rate. Sampling periods of each switch are first expressed in the form $T/p_1 \cdots T/p_n$ (where $p_1 \cdots p_n$ are integers not equal to zero) and then it is shown that each switch with a period T/p can be replaced by a system of switches and advance and delay elements where each switch operates with a sampling period T. In this way, the original sampled-data system can be represented by an equivalent system containing switches operating with the same sampling rate. The general solution of such equivalent systems is outlined in this paper.**

Introduction

IN THE modern technical literature, a great deal of attention has been paid to the analysis and synthesis of feedback systems operating with discrete or sampled data.[1–9] The great majority of the systems described in the literature have one feature in common: they contain a number of switches which operate in synchronism with the same sampling rate. Such systems will be referred to as single-rate sampled systems to be distinguished from multirate sampled systems, defined here as sampled-data systems containing synchronized switches which, however, do not operate with the same sampling rate.

The practical application of multirate systems arises, in many cases, out of problems connected with the analysis and synthesis of standard, single-rate sampled-data systems. Several investigators have used such systems as convenient mathematical analogs. The results they obtained were largely by-products of the work done in other fields of sampled-data theory. Thus, in order to evaluate the output between sampling instants, Linvill and Sittler[6] introduced a fictitious switch operating at twice the sampling rate of the system. Essentially the same approach was later adopted by Lago and Truxal.[7] Sklansky[8] has shown how an error-sampled feedback system can be compensated using continuous networks, by first constructing an approximate model which contained an additional switch operating at a rate equal to n times the sampling rate of the system, n being an integer. He obtained an expression for the closed-form Z transform of the output of the approximate system. The method he used extends ideas of his predecessors to the case where two switches, operating at sampling rates related by an integer, are included in the feedback loop.

In addition to the cases where multirate sampling is used for purely computational purposes, there is a possibility of the actual physical existence of such systems. This may occur in the case of flight-control systems, when a data link computer operates at a rate different from the speed of the radar antenna; or in a situation where multirate sampling is used purposefully to improve the performance of a given system. A sampled-data processor or digital controller operating at a higher rate than the basic sampling rate of the system would exemplify the latter case.[9]

Although sampled-data systems belong to the class of time varying systems, it is possible to treat them very effectively from the point of view of time-invariant or fixed systems through the use of Z transforms. It is shown in this dissertation that multirate sampled systems can be treated also from the point of view of fixed systems, using standard tools of sampled-data mathematics. In this way, the standard methods of Z transforms are extended to cover the case of multirate systems.

Brief Survey of the Field

It has been mentioned already that some theoretical investigations of multirate systems have been carried out in connection with problems arising out of the analysis and synthesis of single-rate systems. The results of these investigations presently will be derived again in a manner which is consistent with the general approach of this paper. In this way the notation, which is largely due to Sklansky, and the basic problem will be introduced. In all examples in this and other sections, switches are assumed to first close simultaneously at time $t=0$.

Considering first the system shown in Fig. 1(a),

* Manuscript received by the PGAC, December 4, 1956. This research was supported by the U. S. Air Force under Contract No. AF 18(600)-677. Presented at WESCON, Los Angeles, Calif., August, 1956.

† Dept. of Elec. Eng., Columbia University, New York 27, N. Y.

[1] L. A. MacColl, "Fundamental Theory of Servomechanisms," D. Van Nostrand Co., Inc., New York, N. Y.; 1945.

[2] W. K. Linvill, "Sampled-data control systems studied through comparison of sampling with amplitude modulation," *Trans. AIEE*, vol. 70, pp. 1779–1788; February, 1951.

[3] J. R. Ragazzini and L. A. Zadeh, "Analysis of sampled-data systems," *Trans. AIEE*, vol. 71, pp. 225–234; November, 1952.

[4] A. R. Bergen and J. R. Ragazzini, "Sampled-data processing techniques for feedback control systems," *Trans. AIEE*, vol. 73, pp. 236–247; November, 1954.

[5] R. H. Barker, "The pulse transfer function and its application to sampling servo systems," *Proc. IEE*, vol. 99, pp. 302–317; December, 1952.

[6] W. K. Linvill and R. W. Sittler, "Extension of conventional techniques to the design of sampled-data systems," 1953 IRE Convention Record, part 1, pp. 99–104.

[7] G. V. Lago and J. G. Truxal, "The design of sampled-data feedback systems," *Trans. AIEE*, vol. 73, pp. 247–253; November, 1954.

[8] J. Sklansky, "Network Compensation of Error-Sampled Feedback Systems," Ph.D. Dissertation, Dept. of Elec. Eng., Columbia University, New York, N. Y.; 1955.

[9] G. M. Kranc, "Compensation of an error-sampled system by a multirate controller," *Trans. AIEE*, vol. 77, pp. 149–159; July, 1957.

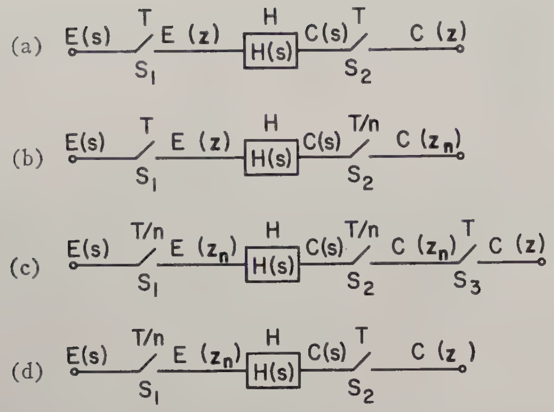

Fig. 1—Multirate open loop systems.

where the switch S_1 operates with the sampling period T, it can be written that

$$C(s) = H(s)E(z) \tag{1}$$

where $C(s)$ is the Laplace transform of the continuous output $c(t)$, $H(s)$ is the Laplace transform of the impulsive response of the network H, $E(z)$ is the Z transform of the input $e(t)$, and $z=\epsilon^{sT}$. The Z transform of $e(t)$ can be denoted also by $Z[e(t)]$ or $Z[E(s)]$ where $E(s)$ is the Laplace transform of $e(t)$. Since $E(z)$ is periodic with respect to $\omega_0=2\pi/T$, Z transforming (1) produces the well-known result:

$$C(z) = Z[C(s)] = Z[H(s)E(z)] = H(z)E(z) \tag{2}$$

where $H(z)=Z[H(s)]$ is referred to sometimes as the "pulsed transfer function." $C(z)$ represents the output sequence of the system shown in Fig. 1(a) where the switch S_2 operates with the same sampling . . . period . . . T as the switch S_1.

Let it be assumed now that the period of the switch S_2 is reduced from T to T/n, n being an integer. This is shown in Fig. 1(b) where the output is sampled at the rate n times higher than the sampling rate at the input. The corresponding Z transform will be denoted by Z_n and the output sequence is given by $Z_n[C(s)]$. Z_n transformation of (1) gives

$$Z_n[C(s)] = Z_n[H(s)E(z)]. \tag{3}$$

Let $C(z_n) \triangleq Z_n[C(s)]$ and $H(z_n) \triangleq Z_n[H(s)]$. Then, since $E(z)$ is periodic in ω_0, and must also be periodic in $n\omega_0$, it can be written that

$$C(z_n) = H(z_n)E(z) = H(z_n)E(z_n{}^n) \tag{4}$$

where z_n is defined as $z^{1/n}=\epsilon^{sT/n}$. It is important to note that $C(z_n)$ is not equal to $C(z)$ with z replaced by z_n, and that since $H(z_n)$ represents the impulsive response of H sampled with the period T/n, it can readily be found from the tables of Z transforms simply by replacing all T by T/n, and all z by z_n in the expression for $H(z)$. On the other hand, $E(z_n{}^n)$ is obtained by replacing every z in the expression for $E(z)$ by $z_n{}^n$.

In the system shown in Fig. 1(c) the switches S_1 and S_2 both operate with the same period T/n. Therefore, it follows from (1) that

$$C(z_n) = H(z_n)E(z_n) \tag{5}$$

where $E(z_n) \triangleq Z_n[E(s)]$ is obtained in the way previously indicated. To obtain the output transform $C(z)$, it is necessary to note that only every nth sample of the sequence $C(z_n)$ can be transmitted through the switch S_3, which operates with the sampling period T. Let $P_n[C(z_n)] \triangleq$ every nth sample of $C(z_n)$. Then

$$C(z) = Z[C(z_n)] = P_n[C(z_n)] = P_n[E(z_n)H(z_n)]. \tag{6}$$

Sklansky[8] has shown that, in general

$$P_n[C(z_n)] \equiv \frac{1}{n}\sum_{k=1}^{n} C(z_n\epsilon^{j(2\pi k/n)}), \tag{7}$$

and therefore,

$$C(z) = \frac{1}{n}\sum_{k=1}^{n} E(z_n\epsilon^{j(2\pi k/n)})H(z_n\epsilon^{j(2\pi k/n)}). \tag{8}$$

It is interesting to note that in (8) the output transform $C(z)$ does not appear any more as a product of the input transform and the pulsed transfer function. In fact, the concept of the pulsed transfer function has no meaning in this case unless a time dependence is introduced. Since the switch S_2 operates with the rate equal to n times the rate of the output samples, its presence is entirely superfluous and therefore it can be replaced by a short circuit without any effect on the output transform $C(z)$ as shown in Fig. 1(c). Thus, one can treat the diagram of Fig. 1(c) as representing a convenient mathematical model of the system in Fig. 1(d).

The procedure outlined above now will be applied to the feedback system shown in Fig. 2(a). The diagram is redrawn in Fig. 2(b) with a superfluous switch, operating with the period T/n, inserted after the network H. It follows from this diagram that

$$E(z) = R(z) - Z[H(z_n)C(z_n)]. \tag{9}$$

On the basis of results previously developed for the open loop case it can also be stated that

$$C(z_n) = G(z_n)E(z_n{}^n). \tag{10}$$

Next, eliminating $C(z_n)$ from (9) and (10) and making use of the periodic properties of $E(z_n{}^n)=E(z)$, it can be shown that

$$E(z) = \frac{R(z)}{1 + Z[H(z_n)G(z_n)]}\cdot \tag{11}$$

Since $Z[H(z_n)G(z_n)]$ implies $P_n[H(z_n)G(z_n)]$, one can make use of the identity stated in (7); also, $E(z)$ and $R(z)$ can be replaced by $E(z_n{}^n)$ and $R(z_n{}^n)$, respectively. Eq. (11) can, therefore, be restated as

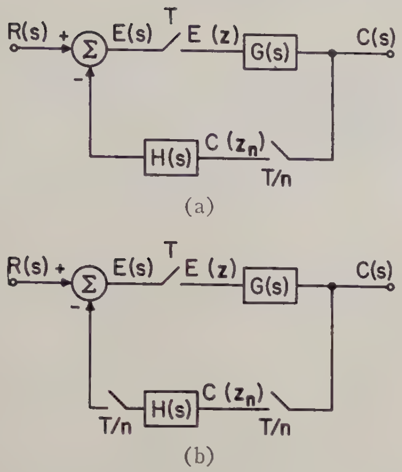

Fig. 2—Multirate feedback system; sampling rates related by an integer.

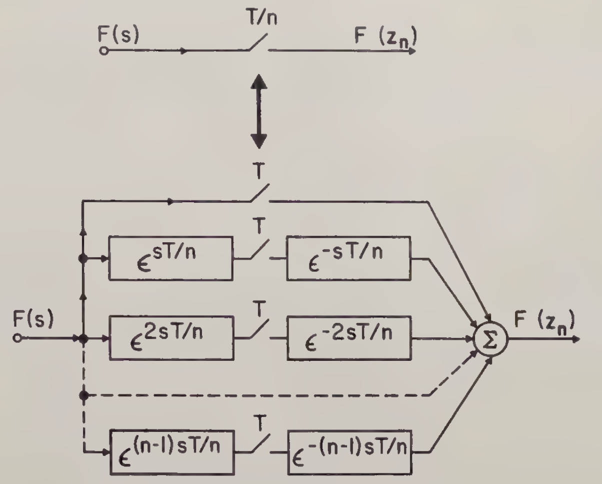

Fig. 3—Switch decomposition diagram.

$$E(z_n{}^n) = \frac{R(z_n{}^n)}{1 + \frac{1}{n}\sum_{k=1}^{n} H(z_n\epsilon^{j2\pi k/n})G(z_n\epsilon^{j2\pi k/n})}. \tag{12}$$

Eliminating $E(z_n{}^n)$ from (10) and (12), one obtains

$$C(z_n) = \frac{R(z_n{}^n)G(z_n)}{1 + \frac{1}{n}\sum_{k=1}^{n} H(z_n\epsilon^{j2\pi k/n})G(z_n\epsilon^{j2\pi k/n})}. \tag{13}$$

Let

$$K(z_n) \overset{\Delta}{=} \frac{C(Z_n)}{R(Z_n{}^n)},$$

then

$$K(z_n) = \frac{G(z_n)}{1 + \frac{1}{n}\sum_{k=1}^{n} H(z_n\epsilon^{j2\pi k/n})G(z_n\epsilon^{j2\pi k/n})}. \tag{14}$$

$K(z_n)$ can be interpreted here as the Z_n transform of the impulsive response of the feedback system shown in Fig. 2(a). It follows from (14) that $K(z_n)$ can be expressed as a ratio of two polynomials in $z_n{}^{-1}$ and therefore in order to determine whether the system shown in Fig. 2 is stable it is sufficient to examine the roots of the denominator. In analogy to the single-rate sampled systems, $K(z_n)$ is a stable transfer function if its denominator vanishes only for values of z_n corresponding to points within the unit circle on the z_n plane.

Introduction to the Switch Decomposition Method

The procedure outlined in the previous section is limited in its application to cases where a sampled-data system contains switches operating at sampling rates whose ratios can be expressed by an integer. A different analytical approach will now be outlined, whose main advantage is that it does not suffer from the above mentioned limitation. Let $F(s)$ be the Laplace transform of the continuous input $f(t)$ to a switch, operating with the sampling period T/n. Then the output sequence is given by Z_n transform of $f(t)$, namely

$$F(z_n) = \sum_{k=0}^{\infty} f(k^T/n)z_n{}^{-k}, \qquad k = 0, 1, 2, \cdots. \tag{15}$$

The same output sequence is obtained from an analogous mathematical model consisting of switches simultaneously operating with a period T, and advance and delay elements as shown in Fig. 3. The validity of this model can be demonstrated by purely physical reasoning. Fig. 4(a) shows a switch S sampling an input $f(t)$ with the period $T/3$ to yield the sequence f_0, f_1, f_2, etc., at its output. In Fig. 4(b) the same function $f(t)$ is sampled by a combination of three switches S_1, S_2, and S_3, in parallel, each of them operating with the period T but with a time delay $T/3$ with respect to one another. Output sequences corresponding to every switch are shown in the diagram and it is obvious that their sum is identically equal to the output of the switch S. It is always possible to simulate the effect of a delayed operation of a switch by advancing the input function, sampling it without a delay, and then delaying appropriately the output sequence in order to place it in the correct time in relation to the rest of the system. Therefore, the operation of the switch, say S_2, can be simulated by placing advance, $\epsilon^{sT/3}$, and delay, ϵ^{-sT3}, elements at the input and output of a switch which closes simultaneously with the switch S. In this way all delayed switches can be replaced by switches without any time delay but with appropriate delay and advance elements, and therefore any switch operating with a period T/n can be replaced by a system of switches operating simultaneously with the period T, as shown in Fig. 3.

Assuming that a sampled-data system to be analyzed contains switches operating with periods $T_1, T_2, \cdots, T_n$, it is always possible to find a number T and a set of integers $p_1, p_2, \cdots, p_n$ such that $T_1 = T/p_1$, $T_2 = T/p_2$, $\cdots$, $T_n = T/p_n$, provided that the ratios of T_1 to T_2 to

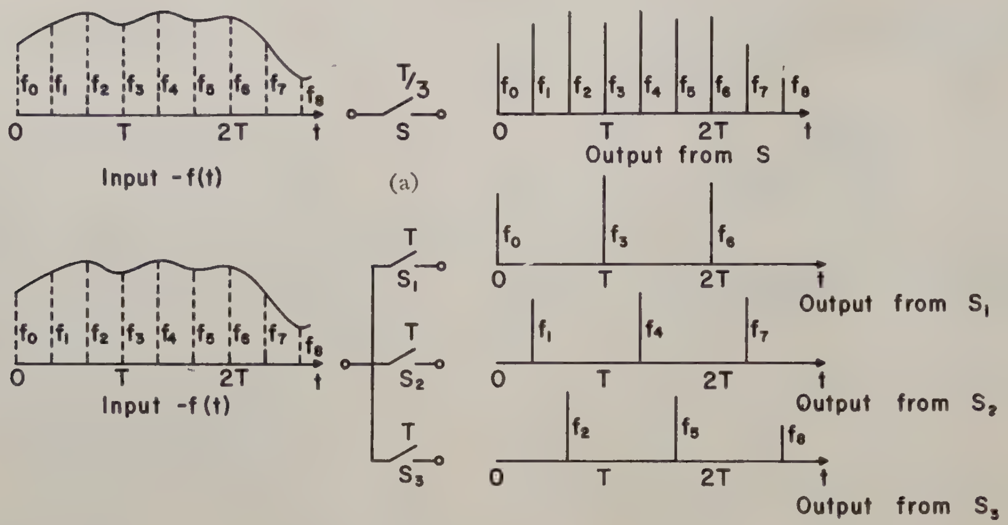

(b)

Fig. 4—Signals in switch decomposition procedure.

$\cdots T_n$ are expressed by rational numbers. This limitation is not serious since we can always approximate an irrational number by a rational one. It follows from the previous discussion that the system under analysis can be replaced by an equivalent mathematical model, with all switches operating with the same period T, thus permitting the use of periodic properties of Z transforms in the formulation of the loop equations. The "switch decomposition technique" described above is the key to the problem under discussion.

General Case

The feedback system shown in Fig. 5(a) will be considered. It contains two switches operating with periods $T_1 = T/p$ and $T_2 = T/q$ where p and q can be any integers (excluding of course zero). Since, as will appear later, the presence of additional switches would only increase the amount of algebra necessary without affecting the method of procedure, this case deals with all the basic points encountered in the general problem. The first step in the procedure is to apply the "switch decomposition technique," thus obtaining the mathematical model shown in Fig. 5(b). The following two equations can be formulated:

$$E(s) = R(s) - B(s) \tag{16}$$

$$\begin{aligned} B(s) = E(z)\{&G(s)H(s) + Z[G(s)\epsilon^{sT/q}]H(s)\epsilon^{-sT/q} \\ &+ Z[G(s)\epsilon^{-2sT/q}]H(s)\epsilon^{-2sT/q} + \cdots \\ &+ Z[G(s)\epsilon^{(q-1)sT/q}]H(s)\epsilon^{-(q-1)sT/q}\} \\ &+ Z[E(s)\epsilon^{sT/p}]\{Z[G(s)\epsilon^{-sT/p}]H(s) \\ &+ Z[G(s)\epsilon^{-sT/p}\epsilon^{sT/q}]H(s)\epsilon^{-sT/q} + \cdots \\ &+ Z[G(s)\epsilon^{-sT/p}\epsilon^{(q-1)sT/q}]H(s)\epsilon^{-(q-1)sT/q}\} + \cdots \\ &+ Z[E(s)\epsilon^{(p-1)sT/p}]\{Z[G(s)\epsilon^{-(p-1)sT/p}]H(s) \\ &+ Z[G(s)\epsilon^{-(p-1)sT/p}\epsilon^{sT/q}]H(s)\epsilon^{-sT/q} + \cdots \\ &+ Z[G(s)\epsilon^{-(p-1)sT/p}\epsilon^{(q-1)sT/q}]H(s)e^{-(q-1)sT/q}\}. \end{aligned} \tag{17}$$

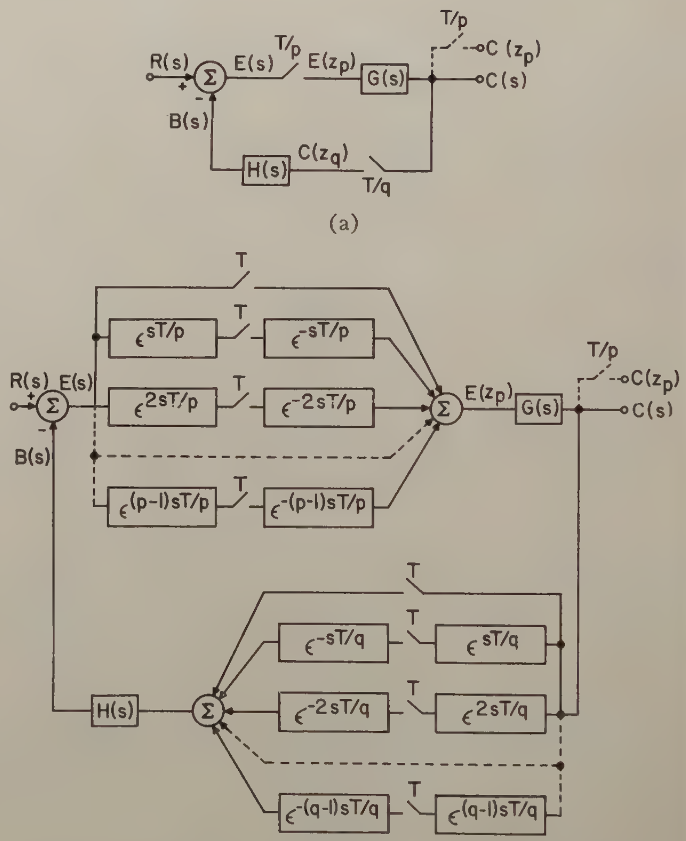

(b)

Fig. 5—Multirate feedback system; sampling rates related by any rational number.

Applying Z_p transformation to both sides of (16) and (17), the following relations are obtained:

$$E(z_p) = R(z_p) - B(z_p) \tag{18}$$

$$\begin{aligned} B(z_p) = E(z)g_1(z_p) &+ Z[E(s)\epsilon^{sT/p}]g_2(z_p) + \cdots \\ &+ Z[E(s)\epsilon^{(p-1)sT/p}]g_p(z_p) \end{aligned} \tag{19}$$

where

$$g_1(z_p) \triangleq \sum_{k=0}^{q-1} Z[G(s)\epsilon^{ksT/q}]Z_p[H(s)\epsilon^{-ksT/q}]$$

$$g_2(z_p) \triangleq \sum_{k=0}^{q-1} Z[G(s)\epsilon^{-sT/p}\epsilon^{ksT/q}]Z_p[H(s)\epsilon^{-ksT/q}]$$

$$\cdots\cdots\cdots\cdots\cdots\cdots$$

$$g_p(z_p) \triangleq \sum_{k=0}^{q-1} Z[G(s)\epsilon^{-(p-1)sT/p}\epsilon^{ksT/q}]Z_p[H(s)\epsilon^{-ksT/q}]. \quad (20)$$

Eliminating $B(z_p)$ from (18) and (19), the following relation is obtained

$$E(z_p) - E(z)g_1(z_p) - Z[E(s)\epsilon^{sT/p}]g_2(z_p) - \cdots - Z[E(s)\epsilon^{(p-1)sT/p}]g_p(z_p) = R(z_p) \quad (21)$$

where $E(z_p)$, $E(z)$, $Z[E(s)\epsilon^{sT/p}]$, $\cdots Z[E(s)\epsilon^{(p-1)sT/p}]$ are unknown terms. To solve (21) for $E(z_p)$ use is made of the identity derived in Appendix I, namely:

$$Z[E(s)\epsilon^{qsT/p}] \equiv \frac{1}{p} z_p^q \sum_{n=1}^{p} \epsilon^{j2\pi q(p-n)/p}E(z_p\epsilon^{j2\pi(p-n)/p}). \quad (22)$$

The above identity permits the expansion of all the unknown terms in (22) into functions of z_p. Performing the indicated expansion and rearranging the terms the following relations are obtained:

$$E(z_p)f_1(z_p) + E(z_p\epsilon^{j2\pi/p})f_2(z_p) + \cdots + E(z_p\epsilon^{j(p-1)/p})f_p(z_p) = R(z_p)$$

or more concisely

$$\sum_{k=1}^{p} E(z_p\epsilon^{j2\pi(k-1)/p})f_k(z_p) = R(z_p) \quad (23)$$

where
$$f_1(z_p) \triangleq 1 + \frac{1}{p}\sum_{l=1}^{p} g_l(z_p)z_p^{l-1}$$

$$f_2(z_p) \triangleq \frac{1}{p}\sum_{l=1}^{p} g_l(z_p)[z_p\epsilon^{j(2\pi/p)}]^{l-1}$$

$$\cdots\cdots\cdots\cdots\cdots\cdots$$

$$f_p(z_p) = \frac{1}{p}\sum_{l=1}^{p} g_l(z_p)[z_p\epsilon^{j2\pi(p-1)/p}]^{l-1}. \quad (24)$$

Eq. (23) is a functional equation with the term $E(z_p\epsilon^{j2\pi(k-1)/p})$, $k=1, 2, \cdots, p$ representing p unknown quantities. Additional $p-1$ equations with *the same unknowns* are readily formed by substituting $z_p\epsilon^{j2\pi/p}$, $z_p\epsilon^{j4\pi/p}$, $\cdots$, $z_p\epsilon^{j2\pi(p-1)/p}$ for z_p in (23). In this way, the following set of p simultaneous equations with p unknowns is obtained:

$$\sum_{k=1}^{p} E(z_p\epsilon^{j2\pi(k-1)/p})f_k(z_p) = R(z_p)$$

$$\sum_{k=1}^{p} E(z_p\epsilon^{j2\pi k/p})f_k(z_p\epsilon^{j2\pi/p}) = R(z_p\epsilon^{j2\pi/p}),$$

$$\cdots\cdots\cdots\cdots\cdots\cdots$$

$$\sum_{k=1}^{p} E(z_p\epsilon^{j2\pi(k+p-2)/p})(f_k(z_p\epsilon^{j2\pi(p-1)/p}) = R(z_p\epsilon^{j2\pi(p-1)/p}). \quad (25)$$

Eq. (25) is solved then, algebraically, for the unknown function $E(z_p)$ and the output sequence is given by the relation:

$$C(z_p) = E(z_p)G(z_p). \quad (26)$$

It is possible to replace loop equations (16) and (17) by equations where the transform of the output rather than the error signal, appears as the unknown. Applying the Z_q transformation to these new equations and making use of the identity (22), $C(z_q)$ is obtained as the solution of the functional equation. Since, in general, this involves q simultaneous equations with q unknowns, this procedure is advantageous whenever q is less than p. It is observed from (20) that in order to evaluate auxiliary functions $g_k(z_p)$ it is necessary to find expressions of the form $Z[F(s)\epsilon^{\alpha sT}]$ and $Z_p[F(s)\epsilon^{\alpha sT}]$. The problem of finding $Z[F(s)\epsilon^{\alpha sT}]$ in a closed form has already been treated in the literature[5,7] in connection with plant delay lags. A brief resume of the procedure to find $Z[F(s)\epsilon^{\alpha sT}]$, and its extension to the case of $Z_p[F(s)\epsilon^{\alpha sT}]$, is given in Appendix II.

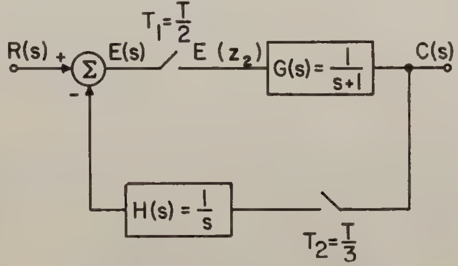

Fig. 6—Illustrative example.

Illustrative Example

The feedback system shown in Fig. 6 is to be considered as an example illustrating some of the points discussed in this section. In this case $T_1=1/2$ sec, $T_2=1/3$ sec, $G(s)=1/(s+1)$, $H(s)=1/s$, and $R(s)=1/s$. To take care of the effect of the small but finite time τ during which switches are assumed to be closed, $G(s)$ and $H(s)$ are defined here as the Laplace transforms of the responses to impulses of strength τ rather than unity. Since T_1 and T_2 can be written as $T/2$ and $T/3$, respectively, with $T=1$ sec, it follows that $p=2$ and $q=3$. Eq. (25) reduces, therefore, to

$$\begin{aligned} E(z_2)f_1(z_2) + E(-z_2)f_2(z_2) &= R(z_2) \\ E(z_2)f_2(-z_2) + E(-z_2)f_1(-z_2) &= R(-z_2) \end{aligned} \quad (27)$$

and $E(z_2)$ is

$$E(z_2) = \frac{R(z_2)f_1(-z_2) - R(-z_2)f_2(z_2)}{f_1(z_2)f_1(-z_2) - f_2(-z_2)f_2(z_2)}. \quad (28)$$

From (24)

$$f_1(z_2) = 1 + \tfrac{1}{2}g_1(z_2) + \tfrac{1}{2}z_2g_2(z_2)$$

and

$$f_2(z_2) = \tfrac{1}{2}g_1(z_2) - \tfrac{1}{2}z_2g_2(z_2) \quad (29)$$

where

$$g_1(z_2) = Z[G(s)]Z_2[H(s)] + Z[G(s)\epsilon^{sT/3}]Z_2[H(s)\epsilon^{-sT/3}] + Z[G(s)\epsilon^{2sT/3}]Z_2[H(s)\epsilon^{-2sT/3}]$$

$$g_2(z_2) = Z[G(s)\epsilon^{-sT/2}]Z_2[H(s)] + Z[G(s)\epsilon^{-sT/6}]Z_2[H(s)\epsilon^{-sT/3}] + Z[G(s)\epsilon^{sT/6}]Z_2[H(s)\epsilon^{-2sT/3}]. \qquad (30)$$

Each term in the above relations can be evaluated making use of Appendix II. Replacing all z by z_2^2 finally obtains the following expressions for $g_1(z_2)$ and $g_2(z_2)$:

$$g_1(z_2) = \frac{1 + \epsilon^{-T/3}z_2^{-1} + \epsilon^{-2T/3}z_2^{-2}}{(1 - \epsilon^{-T}z_2^{-2})(1 - z_2^{-1})}$$

and

$$g_2(z_2) = \frac{(\epsilon^{-T/6} + \epsilon^{-T/2})z_2^{-2} + \epsilon^{-5T/6}z_2^{-3}}{(1 - \epsilon^{-T}z_2^{-2})(1 - z_2^{-1})}; \qquad (31)$$

therefore, noting that $R(z_2) = 1/(1 - z_2^{-1})$,

$$E(z_2) = \frac{1 + (1 - \epsilon^{-T/3})z_2^{-1} + (\epsilon^{-5T/6} - \epsilon^{-T})z_2^{-2} - \epsilon^{-T}z_2^{-3}}{2 + (-1 - \epsilon^{-T} + \epsilon^{-T/3} + \epsilon^{-2T/3} + \epsilon^{-5T/6} + \epsilon^{-T/6})z_2^{-2} + \epsilon^{-1}z_2^{-4}}. \qquad (32)$$

To obtain $C(z_2)$ use can be made of (27) which reads in this case, $C(z_2) = G(z_2)E(z_2)$.

Systems Where at Least One Switch Operates with Period T

In this section a special case of a feedback system, containing at least one switch operating with the sampling period T, is considered. It is assumed that other switches in the system operate with periods T/p_1, $T/p_2, \cdots, T/p_n$, where $p_1, p_2, \cdots, p_n$ can be any integers not equal to zero. The property of the case discussed here is that it is possible to write the loop equations so that the solution of the problem does not lead to functional equations. The loop equations ought to be set up in terms of the unknown variable representing the signal at the input to the switch operating with the sampling period T. Without detracting from the generality of the case under discussion, the feedback system shown in Fig. 7(a) is to be considered. This system contains only three switches, operating with the sampling periods T, T/p, and T/q, p and q being any integers not equal to zero. Applying the "switch decomposition" technique, the equivalent system shown in Fig. 7(b) is obtained. Since the error signal $e(t)$ is the input to the switch which operates with the sampling period T, the loop equations are written in terms of $E(z)$, as the unknown, and they read

$$E(z) = R(z) - B(z) \qquad (33)$$

and

$$B(z) = E(z)\{G_1(z)[G_2(z)H(z) + \cdots + Z[G_2(s)\epsilon^{(q-1)sT/q}]Z[H(s)\epsilon^{-(q-1)sT/q}]] + \cdots + Z[G_1(s)\epsilon^{(p-1)sT/p}][Z[G_2(s)\epsilon^{-(p-1)sT/p}]H(z) + \cdots + Z[G_2(s)\epsilon^{-(p-1)sT/p}\epsilon^{(q-1)sT/q}]Z[H(s)\epsilon^{-(q-1)sT/q}]]\}, \qquad (34)$$

or more concisely

$$B(z) = E(z)\sum_{m=1}^{p}\sum_{k=1}^{q} Z[G_1(s)\epsilon^{(m-1)sT/p}]Z \cdot [G_2(s)\epsilon^{-(m-1)sT/p}\epsilon^{(k-1)sT/q}]Z[H(s)\epsilon^{-(k-1)sT/q}]. \qquad (35)$$

Eliminating $B(z)$ from (33) and (35) the following expression for $E(z)$ is obtained

$$E(z) = \frac{R(z)}{1 + \sum_{m=1}^{p}\sum_{k=1}^{q} Z[G_1(s)\epsilon^{(m-1)sT/p}]Z[G_2(s)\epsilon^{-(m-1/)sTp}\epsilon^{(k-1)sT/q}]Z[H(s)\epsilon^{-(k-1)sT/q}]}. \qquad (36)$$

Finally, since

$$C(s) = G_2(s)Z_p[G_1(s)E(z)] = G_2(s)G_1(z_p)E(z_p^{\,p}), \qquad (37)$$

and therefore

$$C(z_p) = G_2(z_p)G_1(z_p)E(z_p^{\,p}), \qquad (38)$$

it follows that

$$C(z_p) = \frac{R(z_p^{\,p})G_1(z_p)G_2(z_p)}{1 + \sum_{k=1}^{p}\sum_{k=1}^{q} Z[G_1(s)\epsilon^{(m-1)sT/p}]Z[G_2(s)\epsilon^{-(m-1)sT/q}\epsilon^{(k-1)sT/q}]Z[H(s)\epsilon^{-(k-1)sT/q}]}. \qquad (39)$$

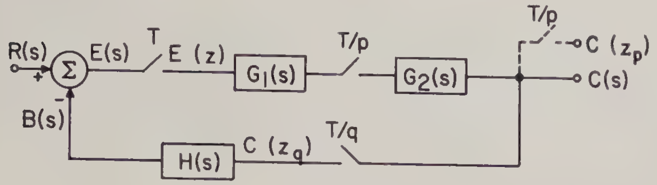

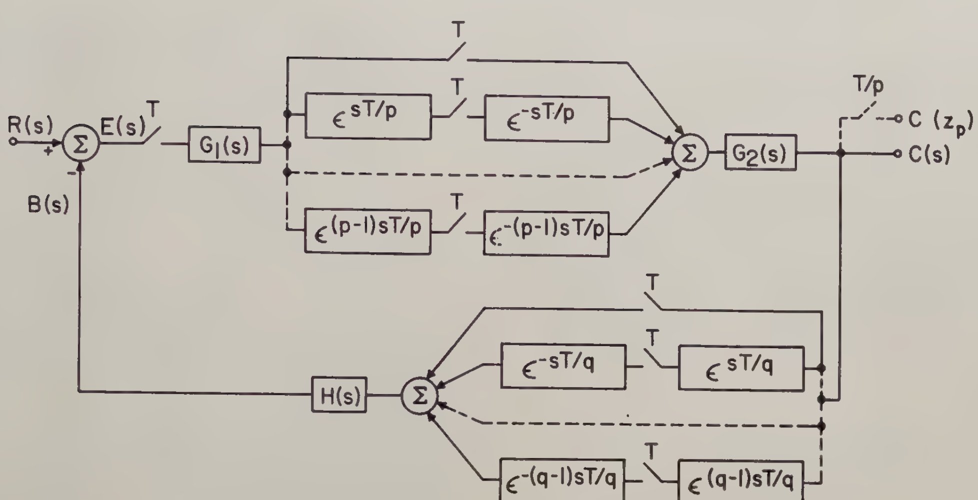

Fig. 7—Multirate feedback system; at least one switch operating with period T.

where $z_p{}^p$ is to replace z in the terms of the denominator.

Conclusion

The analytical technique described here makes it possible to study the behavior of multirate sampled-data systems. It has been shown that, in principle, it is always possible to obtain the closed-form Z transform of the output of such systems and, therefore, standard tools of sampled-data theory could be applied to deal with the problems of stability and performance. The amount of computation necessary to obtain the closed-form Z transforms of the output depends in the feedback cases on the actual values of the integers p and q (assuming that switches with periods T/p and T/q are present). It is obvious that the higher their values, the more computational labor necessary. This becomes especially serious in the general case, where it is shown that in order to obtain the Z transform of the output (p or q, whichever is smaller), simultaneous algebraic equations have to be solved. Computational labor could be reduced by suitable computers or the use of approximations. Thus, it seems reasonable that it is possible to obtain some estimate of the system performance by approximating sampling periods, which lead to high values of integers p and q, and by sampling periods for which the values of p and q are small. In cases when p is large and q is small or vice versa, it seems possible to approximate the ratio p/q (or q/p) by an integer n, thus reducing the system to a case which is easily computable. In this case (sampling periods related by an integer) the amount of computation necessary is independent of the actual values of the sampling periods.

Appendix I

To prove that

$$Z[E(s)\epsilon^{sT/p}] \equiv \frac{1}{p} z_p{}^q \sum_{n=1}^{p} \epsilon^{jq(p-n)2\pi/p} E[z_p \epsilon^{j(p-n)2\pi/p}]$$

where q and p are any positive integer, p not equal to zero.

Proof

Let $e(t) = \mathcal{L}^{-1}E(s)$. Then

$$Z[E(s)\epsilon^{sTq/p}] \stackrel{\Delta}{=} \sum_{k=0}^{\infty} e(kT + q/pT) z^{-k}$$

$$= \frac{1}{T} \sum_{n=-\infty}^{\infty} E\left(s + jn\frac{2\pi}{T}\right) \epsilon^{(s+jn2\pi/T)Tq/p}$$

by Poisson summation rule. Since $\epsilon^{sq/p} = z_p{}^q$, then

$$Z[E(s)\epsilon^{sTq/p}] \equiv \frac{1}{p} z_p{}^q \frac{p}{T} \sum_{n=-\infty}^{\infty} E\left(s + j\frac{np}{Tp} 2\pi\right) \epsilon^{jn2\pi q/p}$$

Since, in general,

$$\sum_{n=-\infty}^{\infty} = \sum_{n=kp} + \sum_{n=kp+1} + \cdots + \sum_{n=kp+p-1}$$

where $k = -\infty, \cdots -1, 0, 1, \cdots \infty$, and p equals any integer not equal to zero, therefore,

$$Z[E(s)\epsilon^{sTq/p}] \equiv \frac{1}{p} z_p{}^q \left\{ \frac{p}{T} \sum_{k=-\infty}^{\infty} E\left(s + jk\frac{2\pi p}{T}\right)\epsilon^{jkq2\pi} + \frac{p}{T}\sum_{k=-\infty}^{\infty} E\left[s + j\left(k + \frac{1}{p}\right)2\pi \frac{p}{T}\right]\epsilon^{j(k+1/p)q2\pi} + \cdots + \frac{p}{T}\sum_{k=-\infty}^{\infty} E\left[s + j\left(k + \frac{p-1}{p}\right)2\pi \frac{p}{T}\right]\epsilon^{j[k+(p-1)/p]q2\pi}\right\}.$$

Since, $\epsilon^{jkq2\pi}=1$, the above relation can be rewritten as

$$Z[E(s)\epsilon^{sTq/p}] \equiv \frac{1}{p} z_p{}^q \left\{ \frac{p}{T} \sum_{k=-\infty}^{\infty} E\left(s + jk\frac{2\pi p}{T}\right) + \epsilon^{j(q2\pi/p)}\frac{p}{T}\sum_{k=-\infty}^{\infty} E\left[s + j\left(k + \frac{1}{p}\right)2\pi \frac{p}{T}\right] + \cdots + \epsilon^{j(p-1/p)q2\pi}\frac{p}{T}\sum_{k=-\infty}^{\infty} E\left[s + j\left(k + \frac{p-1}{p}\right)2\pi \frac{p}{T}\right]\right\},$$

or more concisely,

$$Z[E(s)\epsilon^{sTq/p}] \equiv \frac{1}{p} z_p{}^q \sum_{n=1}^{n=p} \epsilon^{j(q/p)(p-n)2\pi} \cdot \frac{p}{T}\sum_{k=-\infty}^{\infty} E\left[s + j\left(k + \frac{p-n}{p}\right)2\pi \frac{p}{T}\right].$$

To complete the proof it is sufficient to observe that since

$$E(z_p) \triangleq \sum_{k=0}^{\infty} e\left(k\frac{T}{p}\right)z_p{}^{-k} = \frac{p}{T}\sum_{k=-\infty}^{\infty} E\left(s + jk2\pi\frac{p}{T}\right),$$

therefore,

$$\frac{p}{T}\sum_{k=-\infty}^{\infty} E\left[s + j\left(k + \frac{p-n}{p}\right)2\pi \frac{p}{T}\right] = E[z_p\epsilon^{j(p-n/p)2\pi}].$$

Appendix II

In Table I, reproduced from Bergen and Ragazzini,[4] to find $Z[F(s)\epsilon^{\alpha sT}]$ apply the following rules:

1) $0 \leq \alpha < 1$; set $\alpha = \Delta$,

therefore,

$$Z[F(s)\epsilon^{\alpha sT}] = Z[F(s)\epsilon^{\Delta Ts}].$$

2) $\alpha > 1$; set $\alpha = m + \Delta$

where m is a positive integer smaller than α. Therefore,

$$Z[F(s)\epsilon^{\alpha sT}] = Z[F(s)\epsilon^{msT}\epsilon^{\Delta Ts}] = z^m Z[F(s)\epsilon^{\Delta Ts}].$$

3) $-n < \alpha < 0$

where n is a positive integer; set $\alpha = -h + \Delta$. Therefore,

$$Z[F(s)\epsilon^{\alpha sT}] = Z[F(s)\epsilon^{-nsT}\epsilon^{\Delta sT}] = z^{-n}Z[F(s)\epsilon^{\Delta Ts}].$$

TABLE I

Z-Transform Pairs for Functions of the Form $F(s)\epsilon^{\Delta Ts}$, $0 \leq \Delta < 1$

$F(s)\epsilon^{\Delta Ts}$	$Z[F(s)\epsilon^{\Delta Ts}]$
$\frac{1}{s}\epsilon^{\Delta Ts}$	$\frac{1}{1-z-1}$
$\frac{1}{s^2}\epsilon^{\Delta Ts}$	$\frac{\Delta T + Tz^{-1}(1-\Delta)}{(1-z-1)^2}$
$\frac{1}{s+a}\epsilon^{\Delta Ts}$	$\frac{\epsilon^{-a\Delta T}}{1-\epsilon^{-aT}z^{-1}}$
$\frac{a}{s(s+a)}\epsilon^{\Delta Ts}$	$\frac{1-\epsilon^{-a\Delta T}+z^{-1}(\epsilon^{-a\Delta T}-\epsilon^{-aT})}{(1-z^{-1})(1-\epsilon^{-aT}z^{-1})}$

In all cases the problem of finding $Z[F(s)\epsilon^{\alpha sT}]$ reduces to finding the expression for $Z[F(s)\epsilon^{\Delta Ts}]$ from Table I.

To find $Z_p[F(s)\epsilon^{\alpha sT}]$ first note that it can be rewritten as $Z_p[F(s)\epsilon^{\alpha psT/p}]$ and then apply the following rules:

4) $0 \leq \alpha p < 1$; set $\alpha p = \Delta$,

and therefore

$$Z_p[F(s)\epsilon^{\alpha psT/p}] = Z_p[F(s)\epsilon^{\Delta sT/p}].$$

5) $\alpha p \geqq 1$; set $\alpha p = m + \Delta$

where m is a positive integer smaller than αp. Therefore,

$$Z_p[F(s)\epsilon^{\alpha psT/p}] = Z_p[F(s)\epsilon^{msT/p}\epsilon^{\Delta sT/p}] = z_p{}^m Z_p[F(s)\epsilon^{\Delta sT/p}].$$

6) $-n < \alpha p < 0$,

where n is a positive integer. Let $\alpha p = -n + \Delta$ and therefore

$$Z_p[F(s)\epsilon^{\alpha psT/p}] = Z_p[F(s)\epsilon^{-nsT/p}\epsilon^{\Delta sT/p}] = z_p{}^{-n}Z_p[F(s)\epsilon^{\Delta sT/p}].$$

Thus the problem of finding $Z_p[F(s)\epsilon^{\alpha sT}]$ reduces to finding the expression for $Z_p[F(s)\epsilon^{\Delta sT/p}]$. To do this it is sufficient to obtain from Table I, the expression for $Z[F(s)\epsilon^{\Delta Ts}]$ and then to replace every T in it by T/p, and every z by z_p.

Acknowledgment

The author wishes to express his gratitude to Prof. Ragazzini and other members of the Department of Electrical Engineering of Columbia University for many useful discussions.

Statistical Design and Analysis of Multiply-Instrumented Control Systems*

ROBERT M. STEWART†

Summary—It is the purpose of this paper to show how Wiener's linear least-square filter theory may be applied to some common types of multiply-instrumented control systems. By multiply-instrumented control systems are meant those in which more than one sensing instrument is used.

General Solution and Example of Two-Loop Servodesign Problem

Fig. 1 depicts a fairly general form of two-loop servo in which D is a disturbance; ϵ_1 and ϵ_2 are errors in two controlled variables; N_1 and N_2 are noises or errors in *measuring* ϵ_1 and ϵ_2, respectively; Y_{L_1} and Y_{L_2} are two transfer functions characteristic of the "load" being controlled and are ordinarily specified; while Y_{C_1} and Y_{C_2} are the controller transfer functions which are to be designed. If D, N_1, and N_2 are mutually independent stationary random variables, then by straightforward servo and harmonic-analysis techniques it may be shown that the spectral density of ϵ_1 is

$$\left.\begin{aligned}\Phi_{\epsilon_1} &= |1 - X_1 - X_2|^2\{|Y_{L_1}|^2\Phi_D\} + |X_1|^2\Phi_{N_1} \\ &\quad + |X_2|^2\left\{\left|\frac{Y_{L_1}}{Y_{L_2}}\right|^2\Phi_{N_2}\right\} \\ &\text{where} \\ X_1 &= \frac{Y_{L_1}Y_{C_1}}{1 + Y_{L_1}Y_{C_1} + Y_{L_2}Y_{C_2}} \\ &\text{and} \\ X_2 &= \frac{Y_{L_2}Y_{C_2}}{1 + Y_{L_1}Y_{C_1} + Y_{L_2}Y_{C_2}}\end{aligned}\right\}. \quad (1)$$

The mean-square error $\overline{\epsilon_1^2}$ is given by the integral over all frequencies of Φ_{ϵ_1} and the forms of X_1 and X_2 (and, hence, Y_{C_1} and Y_{C_2}) which minimize. It may, in principle, be found for any Φ_D, Φ_{N_1}, and Φ_{N_2} by using the technique outlined by Wiener[1] since (1) corresponds exactly to the two-input filtering problem. An example which has been worked out is one in which acceleration and position measurements are used simultaneously to minimize deviation in position of a load of primarily inertia character.[2] Then, in transform notation,

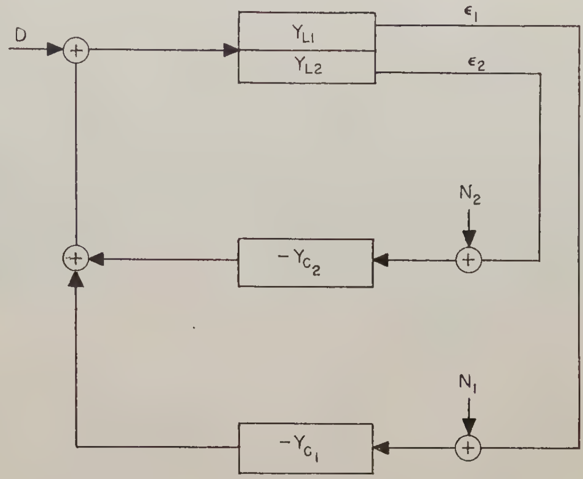

Fig. 1—Dual-loop control system.

$$Y_{L_1} = \frac{1}{p^2}, \qquad Y_{L_2} = 1.$$

For the case in which both instrument errors have flat spectral distributions over the range of frequencies of interest and

$$\Phi_D(\omega) = \frac{\phi_D}{\omega^2},$$

where ϕ_D is a constant, the optimum controller transfer functions turn out to be

$$\left.\begin{aligned}Y_{C_1} &= \frac{1 + \tau p + \left(\frac{\tau^2}{2} - \alpha\right)p^2}{p\left[\left(\sqrt{\frac{\Phi_{N_1}}{\phi_D}} - \beta\right) - \gamma p\right]} \\ Y_{C_2} &= \frac{\alpha + \beta p + \gamma p^2}{p\left[\left(\sqrt{\frac{\Phi_{N_1}}{\phi_D}} - \beta\right) - p\right]} \\ &\text{where} \\ \tau^4 - 8\tau\sqrt{\frac{\Phi_{N_1}}{\phi_D}} - 4\frac{\Phi_{N_1}}{\Phi_{N_2}} &= 0 \qquad \beta = \frac{\tau^2\sqrt{\phi_D\Phi_{N_1}}\Phi_{N_2}}{\left(2 + \tau^2\frac{\phi_D}{\Phi_{N_2}}\right)} \\ \alpha &= \frac{2\frac{\Phi_{N_1}}{\Phi_{N_2}}\left[\tau\sqrt{\frac{\phi_D}{\Phi_{N_1}}} + \frac{\phi_D}{\Phi_{N_2}}\right]}{\left(2 + \tau^2\frac{\phi_D}{\Phi_{N_2}}\right)} \qquad \gamma = \frac{2\Phi_{N_1}\Phi_{N_2}}{\left(2 + \tau^2\frac{\phi_D}{\Phi_{N_2}}\right)}\end{aligned}\right\}. \quad (2)$$

* Manuscript was received by the PGAC, November 10, 1956. The work was supported by the Army Ordnance Corps, ORDCIT Project, under Contract No. DA-04-495-ORD 18. Presented at WESCON, Los Angeles, Calif., August, 1956.

† Jet Propulsion Lab., Calif. Inst. Tech., Pasadena, Calif.

[1] N. Wiener, "Extrapolation, Interpolation, and Smoothing of Stationary Time Series with Engineering Applications," John Wiley & Sons, New York, N. Y.; 1949.

[2] This is a possible representation of the problem of continuously guiding a missile by means of a combination of inertial (accelerometer) and radar data.

It should be clear from this simple example, however, that the utility of the method is limited somewhat by its complexity to the simplest problems. Thus, current and future research effort, applied to methods of simplifying this design technique even at the expense of slightly less precise results, will be extremely useful.

Distortionless Measurements

A technique which has been used frequently in systems, such as the one discussed in the first section, is that of distortionless or "complimentary" measurements. (See for example Ryerson[3] where, however, only the optimum "unrealizable" solution is given.) In this case, there is no contribution to error associated with the signal being measured, but only from the instrument errors.

A typical example is shown in Fig. 2 where S^* is a continuous estimate of the signal S.

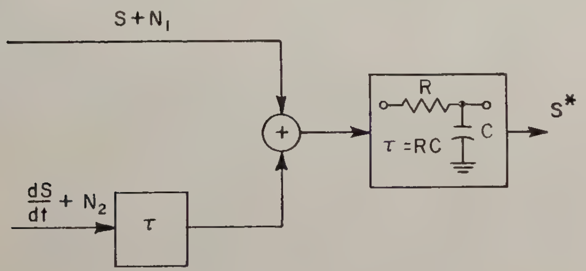

Fig. 2—Typical distortionless system.

This mixing circuit may be shown to be the optimum (in the Wiener sense) distortionless system when the spectral distributions Φ_{N_1} and Φ_{N_2} of N_1 and N_2 are both flat. Then, the optimum time constant is given by:

$$\left.\begin{aligned} \tau_{\text{opt}} &= \left[\frac{\Phi_{N_1}}{\Phi_{N_2}}\right]^{1/2} \\ &\text{and the corresponding mean-square error is:} \\ (\sigma_\epsilon^2)_{\min} &= \frac{1}{2}\left[\Phi_{N_1}\Phi_{N_2}\right]^{1/2} \end{aligned}\right\}. \quad (3)$$

A legitimate comparison with a single-input system often is complicated by various special considerations; but if it is assumed that the spectral distribution of dS/dt, $(\Phi_{\dot{S}})$, is flat, then the ratio of minimum mean-square error with input one to that with two complimentary inputs for the case above is

$$\frac{\sigma_1^2}{\sigma_2^2} = \left[\frac{\Phi_{\dot{S}}}{\Phi_{N_2}}\right]^{1/2}. \quad (4)$$

The ratio on the right is essentially the signal-to-noise ratio of the derivative channel.

Fig. 3 shows two equivalent general methods for mechanizing distortionless dual-input systems with a single frequency-sensitive element.

The error-spectral density in any case is given by

[3] J. L. Ryerson, "Trajectory precision requirements for automatic landing," IRE Trans., vol. ANE-2, pp. 4–10; March, 1955.

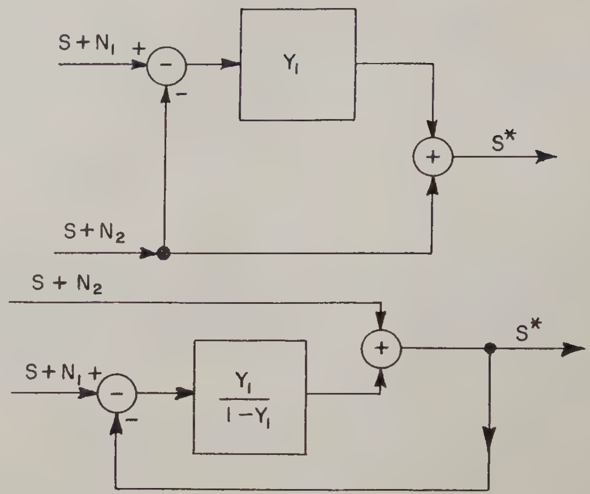

Fig. 3—General distortionless dual-input systems.

$$\Phi_\epsilon = |Y_1|^2\Phi_{N_1} + |1 - Y_1|^2\Phi_{N_2} \quad (5)$$

and the frequency response functions at the output relative to each input are related by

$$Y_1(j\omega) + Y_2(j\omega) = 1. \quad (6)$$

Thus Wiener's solution for the single-input case may be applied to (5) to determine the best form of Y_1 and then, if desired, the corresponding Y_2 can be determined from (6).

An Application of Wiener's Multiple-Input Filtering Theory to Diversity Systems

Another technique of considerable interest in contemporary communication, control, and instrumentation systems is illustrated in Fig. 4.

Wiener's general analysis of such problems shows that, if $S, N_1, N_2, \cdots, N_n$ are mutually independent stationary random time series, the impulsive responses $y_i(\tau)$ of the linear filters which minimize the mean-square error in estimating the "signal" S by S^* satisfy the following simultaneous set of integral equations: $(j=1, 2, \cdots n)$

$$\phi_S(\tau) = \int_0^\infty \left\{[\phi_s(\tau-\sigma)] \sum_{i=1}^n y_i(\sigma) + [\phi_{N_j}(\tau-\sigma)]y_i(\sigma)\right\} d\sigma \qquad \text{for } \tau > 0, \quad (7)$$

where the ϕ terms are autocorrelation functions of the signal and various noises.

These equations are equivalent to:

$$\phi_S(\tau) - \int_{-\infty}^{+\infty} \left\{[\phi_S(\tau-\sigma)] \sum_{i=1}^n y_i(\sigma) + [\phi_{N_j}(\tau-\sigma)]y_j(\sigma)\right\} d\sigma = h_j(\tau) \quad (8)$$

with the understanding that

$$y_i(\sigma) = 0, \qquad \text{for } \sigma < 0, \quad (9)$$

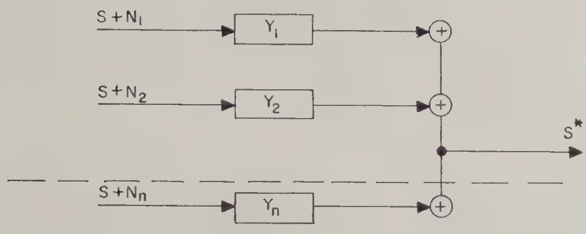

Fig. 4—Diversity system.

(the "realizability" condition) and

$$h_j(\tau) = 0, \qquad \text{for } \tau > 0. \tag{10}$$

Fourier-transforming both sides of (8) then gives

$$\Phi_S(\omega)\left[1 - \sum_{i=1}^{n} Y_i(\omega)\right] - \Phi_{N_j}(\omega)Y_j(\omega) = H_j(\omega) \tag{11}$$

where the Φ's are spectral densities of signal and of the various noises. The Y's are frequency-response functions of the optimum filters having [from (9)] no poles in the lower half-plane of ω, and the H's having [from (10)] no poles in the upper half-plane.[4]

A frequently encountered situation is that in which the noises in the various channels are statistically similar, except possibly for amplitude. Then,

$$\Phi_{N_j} = K_j^2\Phi_{N_0}. \tag{12}$$

Substituting (12) into (11) then gives:

$$\Phi_S\left[1 - \sum^{n} Y_i\right] - K_j^2\Phi_{N_0}Y_j = H_j. \tag{13}$$

Subtracting each side of this equation for arbitrary j from that for $j=1$, gives

$$\Phi_{N_0}[K_j^2Y_j - K_1^2Y_1] = H_1 - H_j. \tag{14}$$

Using Wiener's spectral-factorization theorem,

$$\Phi_{N_0}(\omega) = \overline{\psi(\omega)\psi(\bar{\omega})} = \psi^+\psi^- \tag{15}$$

where ψ^+ and ψ^- have poles and zeroes only in the upper and lower half-planes, respectively. Thus,

$$\psi^+[K_j^2Y_j - K_1^2Y_1] = \frac{H_1 - H_j}{\psi^-}. \tag{16}$$

The left side of (16) can then have poles only in the upper half-plane, while the right side has poles only in the lower half-plane; hence,

$$\psi^+[K_j^2Y_j - K_1^2Y_1] = \text{constant}. \tag{17}$$

[4] Corresponding poles of $s=j\omega$, rather than ω, would be in the right and left half-planes, respectively.

As $\omega \to \infty$, all $|Y_i| \to 0$ since they have been assumed to correspond to well-behaved weighting functions $y_i(\sigma)$ and must, therefore, be Fourier-transformable. Thus,

$$\psi^+[K_j^2Y_j - K_1^2Y_1] \to 0 \tag{18}$$

and, in general,

$$K_j^2Y_j - K_1^2Y_1 = 0 \tag{19}$$

$$Y_j(\omega) = \left(\frac{K_1^2}{K_j^2}\right)Y_1(\omega). \tag{20}$$

Eq. (20) indicates that the optimum system may be mechanized with just one frequency-sensitive element as shown in Fig. 5. This implies the somewhat surprising result that the *optimum bandwidth for each channel is identical, even though the signal-to-noise ratios may be quite different.*

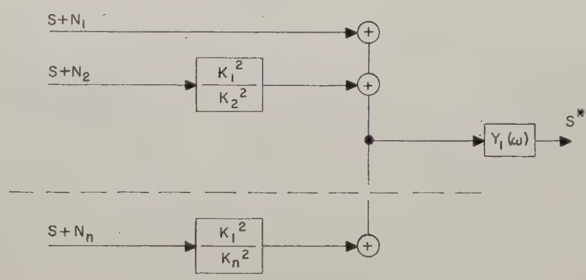

Fig. 5—Possible mechanization.

The best form of Y_1 may be determined as follows: substitution of (20) into (13) gives

$$\Phi_S\left[1 - K_1^2Y_1\sum^{n}\frac{1}{K_i^2}\right] - K_1^2\Phi_{N_0}Y_1 = H_1 \tag{21}$$

or,

$$\Phi_S - [\Phi_S + \Phi_{N_0}']Y_1' = H_1 \tag{22}$$

where

$$\Phi_{N_0}' = \frac{\Phi_{N_0}}{\sum^{n}\frac{1}{K_i^2}} \tag{23}$$

and

$$Y_1' = \left[K_1^2\sum^{n}\frac{1}{K_i^2}\right]Y_1. \tag{24}$$

Eq. (22) may be solved for Y_1' by the method applicable to a *single-input* filter, and then Y_1 may be found from (24).

A Time Domain Synthesis for Optimum Extrapolators*

CARL W. STEEG, JR.†

Summary—**A direct method is presented for the solution of the integral equation for the optimum predictor in terms of the solution to the integral equation for the optimum filter. This method is a means for circumventing the practical difficulties encountered in the actual design of optimum predictors based upon the techniques derived by Wiener. The synthesis procedure is applied in order to simplify the design of extrapolators for use when the prediction interval is a non-negative function of time in contrast to the more conventional situation where prediction is made for a continuously varying instant that is always a fixed number of seconds in the future. The specific example utilized is prediction for a fixed instant that is a continuously decreasing number of seconds in the future. The discussion includes an explanation of a procedure for avoiding the solution of integral equations in the synthesis of optimum extrapolators.**

I. Introduction

One important recent change in communications theory and control-systems engineering is the extension of interest from primarily static performance characteristics to those of a system excited by time functions including actual typical random inputs. Techniques for the design and synthesis of control and communications systems also have been extended to include consideration of both time-domain and frequency-domain characteristics. This paper presents a typical problem in automatic control theory that represents the trend away from frequency-domain methods.

The stationary statistical optimization techniques developed by Wiener[1] and others[2,3] and subsequently extended by Booton[4] to time-varying systems not only have made valuable contributions to communication theory but also have been a stimulus to the application of statistical concepts in the design of other types of systems. In these fields, design often requires that the future value of a signal be predicted. Either of two distinct situations frequently may arise: 1) prediction for a continuously varying instant that is always a fixed number of seconds in the future, 2) prediction for a specific fixed instant that is a continuously decreasing number of seconds in the future. The first situation, which is the classical stationary prediction problem, can be treated by the techniques derived by Wiener.[1] The second situation demands nonstationary theory and is suitable for solution by the theory given by Booton.[4] In each instance, an essential step requires the solution of an integral equation that involves the impulse response of the optimum system. The usual procedure determines the Fourier transform of the impulse response of the physically realizable system through the application of frequency-domain techniques. Although Bode and Shannon[5] have given a thorough discussion of the stationary prediction problem, a similar description of the nonstationary prediction problem has been lacking. These two prediction problems are merely special cases of the general nonstationary problem of predicting over a variable interval.

The application of statistical optimization theory to a system is suitable whenever the input to the system consists of a random signal plus a random noise and if the system is to be designed to produce a response that approximates a desired response. The signal and noise are assumed to be nonstationary in the sense that each are derived by means of a linear time-varying integro-differential operation on white noise. Although this requirement appears to restrict the applicability of the results, it serves both to simplify the mathematical equations and to facilitate the physical description. Furthermore, the only physical systems that are amenable to treatment by existing optimization theory belong to this category of nonstationary systems. The response of the actual system is compared with the result of a desired, time-varying, linear operation upon the signal component of the input, and the resulting difference is called the error. Because time-varying operations are admissible, the entire system must be considered in terms of nonstationary theory,[4] in spite of the assumption that both signal and noise originate as white noise. The optimization criterion is taken as the ensemble-averaged mean-square error, and the characteristics of the physically realizable system are chosen in such a way that this mean-square error is minimized. An assumption inherent in the use of mean-square error is that the system is linear. A linear system belongs to one of two broad categories: 1) systems described by finite-order differential operations and 2) systems not so described. The first class of systems is predominant in automatic control theory. The second class is seldom encountered except in abstract theory of communica-

* Manuscript received by the PGAC, December 12, 1956. The work was supported in part by the U. S. Air Force under contract no. 33(616)-3398, monitored by the Aeronautical Res. Lab., Wright Dev. Ctr., and in part by the Bureau of Ordnance, Dept. Navy, under Contract No. NOrd 16594, both administered through the Div. of Sponsored Res., Mass. Inst. Tech. This paper was presented at WESCON, Los Angeles, Calif., August, 1956.

† Radio Corp. of America, Waltham, Mass.

[1] N. Wiener, "Extrapolation, Interpolation, and Smoothing of Stationary Time Series With Engineering Applications," The Technology Press, Cambridge, Mass.; 1949.

[2] S. O. Rice, "Mathematical analysis of random noise," *Bell Sys. Tech. J.*, vol. 23, pp. 282–332; July, 1944 and vol. 24, pp. 46–156; January, 1945.

[3] H. M. James, N. B. Nichols, and R. S. Phillips, "Theory of Servomechanisms," M.I.T. Rad. Lab. Ser., McGraw-Hill Book Co., Inc., New York, N. Y., vol. 25, 1947.

[4] R. C. Booton, Jr., "An optimization theory for time-varying linear systems with nonstationary statistical inputs," Proc. IRE, vol. 40, pp. 977–981; August, 1952.

[5] H. W. Bode and C. E. Shannon, "A simplified derivation of linear least square smoothing and prediction theory," Proc. IRE, vol. 35, pp. 417–425; April, 1950.

tions. Because the input to the system contains noise, a filtering problem exists even though the desired operation may be merely reproduction of the input. If the result of the desired operation depends upon future values of the input, the fundamental filtering operation must be supplemented by a prediction or, more precisely, an extrapolation. The system described is shown in Fig. 1, where the fundamental dependent variables are defined.

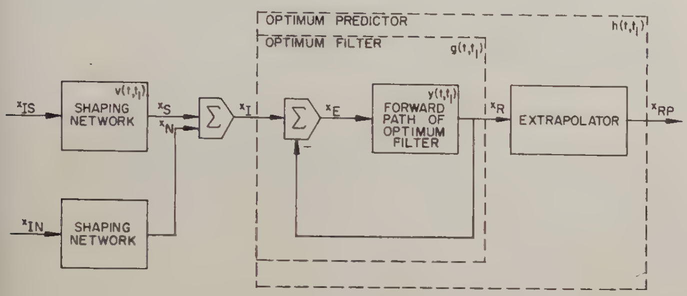

Fig. 1—Block diagram of optimum extrapolator.

Prediction problems usually are classified according to whether nonstationary or stationary statistical optimization theory is needed for the solution. This paper proves the equivalence of the two prediction problems and derives a procedure for determining the optimum predictors. The procedure requires knowledge only of the optimum filter and its impulse response. For this reason, the system designed is called an optimum extrapolator to distinguish it from the conventional optimum predictor. The extrapolator itself is a device that operates upon signals present in the optimum filter to obtain the desired predicted value of the signal component of the input. First, the techniques are established on a rigorous mathematical basis in the time domain. Next, an interpretation of the significance of each signal present in the predictor is given, together with a typical example that includes the results of an analog-computer study. In conclusion, the potential applications and usefulness of the theory are discussed.

II. The Mathematical Theory of Optimum Predictors

If $x_A(t)$ denotes a statistical function, the autocorrelation function γ_{AA} is defined by the ensemble average

$$\gamma_{AA}(t_1, t_2) = \overline{x_A(t_1)x_A(t_2)} \tag{1}$$

where the bar denotes the averaging operation. If the signal is stationary, the autocorrelation function depends only on the difference between t_2 and t_1 and is written in the more familiar form

$$\phi_{AA}(\tau) = \overline{x_A(t_1)x_A(t_1 + \tau)}. \tag{2}$$

Similarly, the cross-correlation function γ_{AB} between two statistical functions x_A and x_B is defined as

$$\gamma_{AB}(t_1, t_2) = \overline{x_A(t_1)x_B(t_2)}. \tag{3}$$

Booton[4] has established that minimization of the mean-square error requires that $u(t, t_2)$, the impulse response of the system defined by the superposition integral,

$$\left.\begin{aligned} x_R(t) &= \int_{-\infty}^{t} u(t, t_2)x_I(t_2)dt_2 \\ u(t, t_2) &= 0, \qquad t_2 > t \end{aligned}\right\}, \tag{4}$$

be determined by the solution to the integral

$$\gamma_{ID}(t_1, t) = \int_{-\infty}^{t} u(t, t_2)\gamma_{II}(t_1, t_2)dt_2, \qquad t_1 < t \tag{5}$$

where γ_{ID} is the cross correlation of the input x_I and the desired response x_D and γ_{II} is the autocorrelation function of the input. To provide consistency for the current development, some slight modifications have been made in the notation used by Booton.[4]

The integral (5) can be reduced to simpler terms according to the characteristics of the input and of the desired response. For example, the function of an optimum filter is to reproduce the signal component of the input; that is, the desired response is the signal. Thus, if the signal and noise components of the input are uncorrelated, the impulse response of the optimum filter $g(t, t_2)$ is determined by the solution to the integral (5) with γ_{ID} equal to γ_{SS},

$$\left.\begin{aligned} \gamma_{SS}(t_1, t_3) &= \int_{-\infty}^{t_3} g(t_3, t_2)\gamma_{II}(t_1, t_2)dt_2, \quad t_1 < t_3, \\ g(t_3, t_2) &= 0 \qquad\qquad t_3 < t_2. \end{aligned}\right\} \tag{6}$$

Similarly, the desired response of an optimum predictor is equal to the signal evaluated at some future time $t+\alpha$, and the impulse response of the optimum predictor $h(t, t_2)$ is obtained by the solution to the integral

$$\left.\begin{aligned} \gamma_{SS}(t_1, t + \alpha) &= \int_{-\infty}^{t} h(t, t_2)\gamma_{II}(t_1, t_2)dt_2, \quad t_1 < t, \\ h(t, t_2) &= 0, \qquad\qquad t < t_2, \end{aligned}\right\} \tag{7}$$

where α can be any nonnegative function of t. If the substitution $t_3 = t + \alpha$ is made, (7) becomes

$$\left.\begin{aligned} \gamma_{SS}(t_1, t_3) &= \int_{-\infty}^{t_3-\alpha} h(t_3 - \alpha, t_2)\gamma_{II}(t_1, t_2)dt_2, \\ &\qquad\qquad t_1 < t_3 - \alpha, \\ h(t_3 - \alpha, t_2) &= 0, \qquad\qquad t_3 < t_2 + \alpha. \end{aligned}\right\} \tag{8}$$

Because the latter part of (8) holds, the upper limit on the integral can be written t_3 rather than $t_3 - \alpha$. Thus,

$$\gamma_{SS}(t_1, t_3) = \int_{-\infty}^{t_3} h(t_3 - \alpha, t_2)\gamma_{II}(t_1, t_2)dt_2, \; t_1 < t_3 - \alpha. \tag{9}$$

Design procedures[1] for determining the optimum filter provide the necessary means for ascertaining the function $g(t_3, t_2)$. The following development describes a method for the determination of the optimum pre-

dictor when only the impulse response of the optimum filter is known. The response x_R of the optimum filter is given by

$$x_R(t) = \int_{-\infty}^{t} g(t, t_1)x_I(t_1)dt_1 \tag{10}$$

where $g(t, t_1)$ satisfies (6). Similarly, the response of the optimum predictor can be written

$$x_{RP}(t) = \int_{-\infty}^{t} h(t, t_1)x_I(t_1)dt_1 \tag{11}$$

where $h(t, t_1)$ satisfies (7).

Although this equation often is used as a basis for the design of optimum predictors, a slightly different configuration for the system offers advantages in the interpretation of the duality between the stationary and nonstationary prediction problems. The configuration preferred for this purpose is shown in Fig. 1 where the straight transmission corresponding to $g(t, t_1)$ is replaced by an equivalent unity-feedback transmission involving $y(t, t_1)$, the impulse response of the forward path. The configuration represents a significant departure from the techniques used in the references. Reasons for the choice of this configuration are emphasized in the development of Appendix I. The following definitions, indicated in Fig. 1, are convenient:

$$x_E(t) = x_I(t) - x_R(t) \tag{12}$$

and

$$\begin{aligned} x_R(t) &= \int_{-\infty}^{t} y(t, t_1)x_E(t_1)dt_1 \\ &= \int_{-\infty}^{t} y(t, t_1)[x_I(t_1) - x_R(t_1)]dt_1. \end{aligned} \tag{13}$$

To be physically realizable, the impulse response of the forward path $y(t, t_1)$ is zero for $t_1 > t$.

The remainder of this section is concerned with establishing the validity that, under the condition that the noise component of the input is white,

$$x_{RP}(t) = \int_{-\infty}^{t} y(t + \alpha, t_1)x_E(t_1)dt_1 \tag{14}$$

relates the response of the optimum predictor to the error signal of the optimum filter and to the impulse response of the forward path of the optimum filter.

Because

$$\begin{aligned} x_R(t + \alpha) &= \int_{-\infty}^{t+\alpha} y(t + \alpha, t_1)x_E(t_1)dt_1 \\ &= \int_{-\infty}^{t} y(t + \alpha, t_1)x_E(t_1)dt_1 \\ &\quad + \int_{t}^{t+\alpha} y(t + \alpha, t_1)x_E(t_1)dt_1, \end{aligned} \tag{15}$$

the expression (14), for the response of the optimum predictor, indicates that the predictor response approximates the future value of the filter response by the omission of the integral

$$\int_{t}^{t+\alpha} y(t + \alpha, t_1)x_E(t_1)dt_1. \tag{16}$$

This integral requires values of the error in the future; that is, for t_1 in the interval between t and $t+\alpha$. Because such values are not known, the integral must be neglected in the determination of future values of the input. This conclusion can be reached on a more rigorous basis by the argument given in Appendix I.

III. The Time-Domain Synthesis Procedure

The function of the optimum predictor is derived in the preceding section, where the output of the predictor is proved to be given by

$$x_{RP}(t) = \int_{-\infty}^{t} y(t + \alpha, t_1)x_E(t_1)dt_1 \tag{17}$$

where $y(t, t_1)$ is the impulse response of the forward path of an optimum filter and $x_E(t)$ is the error signal in the filter. In an important class of optimum filters, the impulse response $y(t, t_1)$ can be written in the form

$$y(t, t_1) = \sum_{j=0}^{n} c_j(t_1)\phi_j(t); \tag{18}$$

that is, the impulse response, or kernel, is separable into the sum of the products of functions of t and t_1 only. For this special, but dominant class, the optimum filter can be expressed in terms of a differential operator involving $x_R(t)$, $x_E(t)$ and their derivatives. The use of mean-square error as a criterion restricts the filter to a linear form and virtually all such forms are described by impulse responses that are separable. When the impulse response is separable, an expression equivalent to (17) can be established in order to simplify the design of the optimum predictor. The expression depends upon the impulse response of the optimum filter and involves only current values of $x_R(t)$, $x_E(t)$ and their derivatives in order to determine future values of the filter response. For this reason, the operation is called extrapolation, and the resultant system is termed an optimum extrapolator.

The equivalent expression for the integral (17) is obtained most easily from certain identities derived in the theory of ordinary differential equations.[6] Because these results are apt to be unfamiliar to engineers, the following discussion includes somewhat greater detail than might be required in establishing the desired equivalence. However, some facility in the manipulation of the following equations is useful in applications such as the example given at the end of Section IV.

[6] E. A. Coddington and N. Levinson, "Theory of Ordinary Differential Equations," McGraw-Hill Book Co., Inc., New York, N. Y.; 1955.

If the coefficients of

$$L(x) = \sum_{i=0}^{n} a_i(t) \frac{d^i x}{dt^i} = 0 \tag{19}$$

are all finite, single-valued, and continuous throughout a prescribed time interval, the fundamental existence theorems for the solutions to ordinary differential equations prove that there exists a unique solution $x(t)$ such that $x(t)$ and its first $n-1$ derivatives assume a set of arbitrarily assigned values $x_0, x_0^{(1)}, \cdots, x_0^{(n-1)}$, when $t=t_0$, and such that $x(t)$ may be developed as a Taylor's series convergent in a certain interval around t_0.[6–8]

Any linearly-independent set of n solutions to (19) is said to form a fundamental set or fundamental system of solutions. Although there is an infinite number of such sets, one particular fundamental set is of special importance because of its simplicity. Members of this particular fundamental set are designated as $f_i(t, t_0)$, $i=0, 1, \cdots, n-1$, and these particular solutions to (19) are defined uniquely by the conditions

$$\left. \frac{d^j}{dt^j} f_i(t, t_0) \right|_{t=t_0} = \delta_{ij}, \quad j = 0, 1, \cdots, n-1, \tag{20}$$

where δ_{ij} is the Kronecker delta, which assumes the value 1 when $i=j$ and is zero otherwise. Consequently, a unique solution to (19) is expressible as

$$\begin{aligned} x(t) &= x(t_0)f_0(t, t_0) + x^{(1)}(t_0)f_1(t, t_0) + \cdots \\ &\quad + x^{(n-1)}(t_0)f_{n-1}(t, t_0) \\ &= \sum_{i=0}^{n-1} x^{(i)}(t_0)f_i(t, t_0). \end{aligned} \tag{21}$$

Therefore, the derivation of the n fundamental solutions $f_i(t, t_0)$ is sufficient for obtaining either the general solution to (19) or a particular solution satisfying preassigned conditions. The solution defined by (21) describes the behavior that is usually called the transient.

The condition expressed by (20) implies that the leading term of $f_i(t, t_0)$ is $(t-t_0)^i/i!$ and that no terms in $(t-t_0)^{i+1}, \cdots, (t-t_0)^{n-1}$ are present in the expansion. The usual method for the solution of (19) is to assume that

$$i!f_i(t, t_0) = (t - t_0)^i \left[1 + \sum_{j=n-i}^{\infty} a_{ij}(t - t_0)^j \right], \tag{22}$$

[7] This statement of the existence theorems is valid only if t_0 is not a singular point of the differential equation. Under the conditions outlined the only singular points that can occur within the prescribed interval are the zeros of the leading coefficient $a_n(t)$. All other points are ordinary points. A singular point is defined as a pair of values of x and t for which the solution to (29) either is discontinuous, is not unique, or does not exist. Because such conditions arise infrequently in control-systems applications, the assumption is made here that $a_n(t)$ is different from zero throughout the entire time interval during which extrapolation operates.

[8] E. L. Ince, "Ordinary Differential Equations," Dover Publications, New York, N. Y.; 1944.

to substitute the series in the differential equation, to arrange the resulting expression in ascending powers of $(t-t_0)$, and to equate the coefficients of like powers of $(t-t_0)$ to zero. By this procedure, a set of simultaneous linear algebraic equations in the coefficients a_{ij} is obtained. The relations between coefficients are called recurrence equations. The complete procedure can be circumvented in many practical problems, such as constant-coefficient differential equations.

The fundamental existence theorems for ordinary differential equations provide a basis for the prediction of many analytical functions. If T is a value of t within an interval that contains no singular points, then, by (21)

$$x(t) = \sum_{i=0}^{n-1} x^{(i)}(T)f_i(t, T). \tag{23}$$

Because relations between t and T are bilateral,

$$x(T) = \sum_{i=0}^{n-1} x^{(i)}(t)f_i(T, t); \tag{24}$$

that is, the value of x at any particular time is expressible continuously as a time-weighted sum of values of x and its derivatives at any other time. Thus, in particular, if $T=t+\alpha$,

$$x(t + \alpha) = \sum_{j=0}^{n-1} x^{(j)}(t)f_j(t + \alpha, t). \tag{25}$$

The definition of the fundamental set is such that, for α equal to zero, (25) reduces to the identity that $x(t)$ is equal to $x(t)$. As α increases from zero, increased weight is attached to the derivatives of x.

For constant-coefficient equations which are invariant under translations in time, the members of the fundamental set are functions of the difference between the two variables only. Hence,

$$f_i(t, t_0) = f_i(t - t_0) \tag{26}$$

for constant-coefficient systems, and the prediction formula becomes

$$x(t + \alpha) = \sum_{j=0}^{n-1} x^{(i)}(t)f_i(\alpha). \tag{27}$$

If prediction is made over a fixed interval; that is, if the value of the function is desired for a continuously varying instant that is always a fixed number of seconds in the future, the prediction formula is interpreted as applying constant weights to current values of the derivatives of the function to be predicted. Consequently, the origin of the weighting functions encountered in the Wiener theory of stationary prediction is explained.

Eq. (24) leads to interesting and useful identity among members of the fundamental set. Because the left-hand member does not depend on the current value of t, differentiation with respect to t yields

$$0 = \sum_{j=0}^{n-1} x^{(j+1)} f_j(T, t) - \sum_{j=0}^{n-1} x^{(j)}(t) \frac{d}{dt} f_j(T, t)$$

$$= x(t) \frac{d}{dt} f_0(T, t) + \sum_{j=0}^{n-1} x^{(j)}(t) \left[f_{j-1}(T, t) + \frac{d}{dt} f_j(T, t) \right]$$

$$+ f_{n-1}(T, t) x^{(n)}(t). \tag{28}$$

Because $x(t)$ is derived from (19), the nth-order differential (19) and (28) must differ at most by a multiplicative factor, designated as $K(T, t)$. For example, comparison of the coefficients of the nth derivative results in

$$f_{n-1}(T, t) = a_n(t) K(T, t). \tag{29}$$

The function $K(t, t')$ is called the unilateral Green's function[9] for the operator L and is important in the solution of differential equations with forcing functions.

Comparison of the coefficients of lower derivatives results in the further identities

$$\left.\begin{aligned} a_j(t) K(T, t) &= f_{j-1}(T, t) + \frac{d}{dt} f_j(T, t), \\ & \qquad j = 1, 2, \cdots, n-1 \\ a_0(t) K(T, t) &= \frac{d}{dt} f_0(T, t). \end{aligned}\right\} \tag{30}$$

The foregoing equations are the basis for a recurrence relation that permits the members of the fundamental set to be expressed in terms of the single function $K(T, t)$.

$$f_j(T, t) = \sum_{i=j}^{n-1} (-1)^{i-j} \frac{d^{i-j}}{dt^{i-j}} [a_{i+1}(t) K(T, t)]. \tag{31}$$

Hence, knowledge of the function $K(t, t')$ is adequate to obtain the general solution to (19).

The Green's function $K(t, t')$ and the impulse response or weighting function $k(t, t')$ are equal throughout the interval of definition of the latter; that is,

$$\begin{aligned} k(t, t') &= K(t, t') \qquad t' < t \\ k(t, t') &= 0 \qquad\qquad\quad t' \geqq t. \end{aligned} \tag{32}$$

The description of linear control systems necessarily contains more complex equations than linear homogeneous differential equations. One complicating factor is that most central systems utilize variations in a forcing function to achieve control. Hence, the preceding equations, which are a basis for the prediction of the transient component of the solution to a differential equation, must be augmented by formulas that include the effects of the steady-state component of the solution, a component that arises from the presence of a forcing term.

[9] K. S. Miller, "Properties of impulse responses and Green's functions," IRE Trans., vol. CT-2, pp. 26–31; March, 1955.

The desired formulas can be derived in the following way. The differential

$$L(x_R) = \sum_{i=0}^{n} a_i(t) \frac{d^i x_R}{dt^i} = x_f(t) \tag{33}$$

has the function $K(T, t)$ as an integrating factor. Multiplication of both sides of (33) by $K(T, t)$ and integration between the limits t and T yield, according to (28),

$$\sum_{i=0}^{n-1} f_i(T, t) x_R^{(i)}(t) = x_R(T) - \int_t^T K(T, t') x_f(t') dt', \tag{34}$$

or

$$x_R(T) = \sum_{i=0}^{n-1} f_i(T, t) x_R^{(i)}(t) + \int_t^T K(T, t') x_f(t') dt'. \tag{35}$$

Whenever the forcing function $x_f(t)$ is known over the interval to T, (35) provides an exact prediction formula. Such information usually is not available, and only estimates of the value of $x_f(t)$ over this interval can be obtained. In Section II of this paper, it is shown that for optimum statistical prediction a "best" estimate of $x_f(t)$ is zero. In virtually every case of statistical optimization the filter response is obtained from a combined integrodifferential operation on the filter error signal; that is, the forcing function $x_f(t)$ is derived from a differential operation on the variable $x_E(t)$. In such cases, the differential operations

$$L(x_R) = \sum_{i=0}^{n} a_i(t) \frac{d^i x_R}{dt^i} = \sum_{j=0}^{m} b_i(t) \frac{d^i x_E}{dt^i} = M(x_E) \tag{36}$$

where $m < n$ can be used to describe the filter. If again the function $K(T, t)$ is used as an integrating factor, the prediction

$$x_R(T) = \sum_{i=0}^{n-1} f_i(T, t) x_R^{(i)}(t) + \int_t^T K(T, t') \left[\sum_{i=0}^{m} b_i(t') \frac{d^i x_E}{dt'^i} \right] dt' \tag{37}$$

can be derived. The integral in (31) can be simplified, if the interchange of summation and integration is allowable by successive integration by parts. This process is tedious and not repeated here. The results of the integration by parts are expressible in the form

$$x_R(T) = \sum_{i=0}^{n-1} f_i(T, t) x_R^{(i)}(t) - \sum_{i=0}^{m-1} g_i(T, t) x_E^{(i)}(t) + \int_t^T K^*(T, t') x_E(t') dt' \tag{38}$$

where

$$K^*(T, t') = \sum_{i=0}^{m} (-1)^i \frac{d^i}{dt'^i} [b_i(t') K(T, t')]$$

$$g_i(T, t') = \sum_{j=n-m+1}^{n-1} C_{ij} f_j(T, t) \quad i = 0, \cdots, m-1. \tag{39}$$

The definition of unilateral Green's function usually is extended to include $K^*(T, t')$ as the impulse response of (36). Prediction often involves neglecting the integral term in (37), a process equivalent to the assumption that $x_E(t')$ is zero for t' between t and T. The remaining terms in (37) can be recombined by the aid of (39) into the form

$$x_R(T) = \sum_{i=0}^{n-1} f_i(T, t)x_R^{(i)}(t) - \sum_{i=0}^{m-1} \sum_{j=n-m+i}^{n-1} C_{ij}(t)f_j(T, t)x_E^{(i)}(t)$$

$$= \sum_{i=0}^{n-1} f_i(T, t)x_R^{(i)}(t) - \sum_{i=n-m}^{n-1} \sum_{j=0}^{i+m-n} C_{ij}(t)f_i(T, t)x_E^{(j)}(t)$$

$$= \sum_{i=0}^{n-1} f_i(T, t)x_i(t) \tag{40}$$

where

$$x_i(t) = x_R^{(i)}(t), \qquad i = 0, \cdots, n-m-1$$

$$= x_R^{(i)}(t) - \sum_{j=0}^{i+m-n} C_{ji}(t)x_E^{(j)}(t)$$

$$i = n-m, \cdots, n-1. \tag{41}$$

Frequently, the quantities $x_i(t)$ can be identified with the outputs of the energy storage elements in the filter. Unfortunately, the quantities $C_{ij}(t)$, which are combinations of the functions $a_i(t)$ and $b_i(t)$, are difficult to determine, except for rudimentary systems. However, the weighting functions $f_i(T, t)$ depend only on the operator L, which is related to the signal shaping in an optimum filter and often can be found by standard methods.

If $K^*(t, t')$ is identified with the forward path of the optimum filter, then $y(t, t')$ is equal to $K^*(t, t')$ and (38) can be written

$$\int_{-\infty}^{t} y(\tau, t_1)x_E(t_1)dt_1 = \sum_{i=0}^{n-1} f_i(\tau, t)x_R^{(i)}$$

$$- \sum_{i=0}^{m-1} g_i(\tau, t)x_E^{(i)}. \tag{42}$$

This expression is a mathematical identity for all values of $\tau \geqq t$. Thus, in particular, if $\tau = t + \alpha$,

$$x_{RP}(t) = \sum_{i=0}^{n-1} f_i(t+\alpha, t)x_R^{(i)} - \sum_{i=0}^{m-1} g_i(t+\alpha, t)x_E^{(i)}. \tag{43}$$

This expression provides a means for extrapolating over any nonnegative prediction interval α. A convenient form for α is a triangular wave of high frequency. Use of such a prediction interval would permit oscilloscope display of continuous estimates of the future values of a function.

The synthesis procedure for the optimum extrapolator now can be summarized in the following steps:

1) From the separable impulse response of the forward path of the optimum filter $y(t, t_1)$, determine the differential equation.
2) Find the impulse response $K(\tau, t)$ of the operator on x_R.
3) Find the functions $f_j(\tau, t)$ and $g_j(\tau, t)$ in terms of $K(\tau, t)$ and the coefficients of the differential operator.
4) Form (42) for the extrapolated response.

Relationships derived in this section are not restricted to application in optimum systems alone but may be employed whenever analytic extrapolation of any function generated by an integrodifferential operation is required. One such application is found in final value control systems.[10]

IV. Discussion

The significance of the foregoing development may be elucidated by a thorough discussion of the physical meaning of the blocks in the diagram of Fig. 1. For the purposes of theoretical investigations, substantial significance can be attached to the mathematical results, which comprise a method for the solution to the prediction integral (7) when only the solution to the filter integral (6) is known. However, a more complete understanding of the operation of the filter and the extrapolator enhances the usefulness of the method in practical applications. For such a discussion, it is convenient to assume that the quantities x_{IS} and x_{IN} shown in Fig. 2 are white noise and that the network shaping x_{IS} into

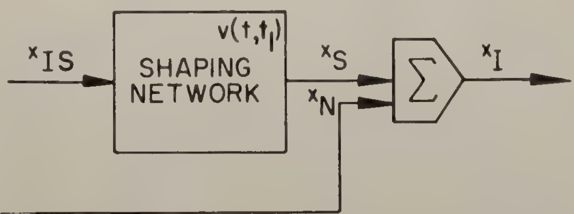

Fig. 2—Input shaping when X_n is white noise.

the signal component of the input x_S has an impulse response $v(t, t_1)$. Thus,

$$x_S(t) = \int_{-\infty}^{t} v(t, t_1)x_{IS}(t_1)dt_1. \tag{44}$$

If τ is a time greater than t, the present time, then

$$x_S(\tau) = \int_{-\infty}^{\tau} v(\tau, t_1)x_{IS}(t_1)dt_1. \tag{45}$$

However, to evaluate this integral, values of x_{IS} would be required over the interval between t and τ. Because these values are not known at time t, the best physically realizable approximation to (45) is

$$x_{SP}(\tau) = \int_{-\infty}^{t} v(\tau, t_1)x_{IS}(t_1)dt_1. \tag{46}$$

[10] C. W. Steeg and M. V. Mathews, "Final-value controller synthesis," IRE Trans., vol. AC-2, pp. 6–16; February, 1957.

This portion of the integral (45) omitted in writing (46) is

$$x_S(\tau) - x_{SP}(\tau) = \int_t^\tau v(\tau, t_1)x_{IS}(t_1)dt, \qquad (47)$$

which vanishes as t approaches τ. The integral (47) also would vanish, making the approximation exact if x_{IS} were identically zero over the interval between t and τ. Because x_{IS} is assumed to be white noise with zero mean, the vanishing of the integral (47) is equivalent to replacing x_{IS} by its mean value (zero) over the interval $t \leq t_1 \leq \tau$. This conclusion is tantamount to the statement that the best prediction of white noise with zero mean is no prediction at all.

If the shaping network were available for physical measurement of both x_S and x_{IS} and their derivatives, the integral (46) could be replaced by its equivalent expression, analogous to (40), and the prediction made on the basis of these measurements. However, this procedure must be abandoned in many physical problems such as an automatic radar-tracking system where the shaping network is a remotely located physical body, and only the output x_S which might represent the position of the aircraft being tracked is available for measurement. Because such measurements inevitably are corrupted by noise, both filtering and prediction must be conducted on the basis of an error-minimization criterion and associated optimization theory.

The operation of the filter can be described in the following terms. The input to the filter is the noise-corrupted signal, and the response of the filter is the best approximation to the signal component of the input in the sense of least-mean-square error. If the noise component of the input is white, then the error signal x_E is also white and has the same autocorrelation function as the noise. (This result is established in Appendix II.) Consequently, the operation of the forward path of the filter, as shown in Fig. 3, is to recreate the signal component out of white noise. But this operation is precisely the same as that of the shaping network which produces the signal originally. This reconstruction process can be regarded as composed of the three following steps: 1) a gain to change the amplitude of x_E into the amplitude of x_{IS}, 2) a network to change x_C into a signal x_A with the optimum approximation to the time function of x_{IS}, and 3) an exact model of the shaping network. Of these three steps, only the second involves any difficulty. Ideally, the second step would convert x_C into x_{IS}. The autocorrelation function of x_C is the same as the autocorrelation function of x_{IS}, but the corresponding time functions are different; therefore, this conversion cannot be performed exactly since neither time function is known. Hence, an error criterion, in this case, least-mean-square error, is used to minimize the difference between x_{IS} and x_A as functions of time. The combination of the results of steps 2) and 3) may be regarded as the optimized system model; that

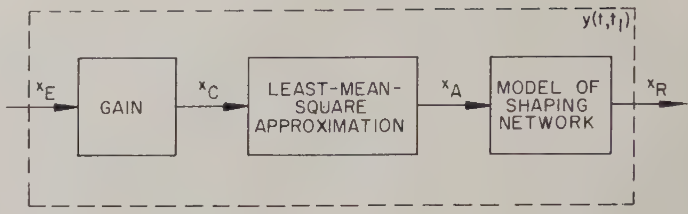

Fig. 3—Alternate diagram for forward path of optimum filter.

is, the model of the shaping network optimized with respect to minimization of the mean-square error.

Because the forward path does represent a model of the shaping network, prediction can be made on the basis of signals physically existing in the filter, which is accessible for measurements, rather than on the actual system itself. This prediction is made by means of the relation

$$x_{RP}(\tau) = \int_{-\infty}^{t} y(\tau, t_1)x_E(t_1)dt_1 \qquad (48)$$

or its associated equivalent (41). Relation (48) is used instead of (46), which cannot be achieved, and the operation of (41) is called extrapolation.

V. Conclusion

This paper presents a direct method for the time-domain synthesis of optimum extrapolators. The extrapolators are optimum predictors that require merely the knowledge of design principles for optimum filters. To indicate the universal applicability of the synthesis procedure, the method is used for the simplified design of predictors for two distinct situations: 1) prediction for a continuously varying instant that is always a fixed number of seconds in the future, and 2) prediction for a specific fixed instant that is a continuously decreasing number of seconds in the future. The method is discussed on the basis of uncorrelated signal and noise, both of which are derived from white-noise sources, although these restrictions can be removed easily by arguments analogous to the ones given by Bode and Shannon[5] in their discussion of prediction theory. Furthermore because the extrapolator design is independent of the error criterion, the synthesis procedure can be used for the simplified design of other systems such as predictors that use finite-memory filters.[11]

The hypothesis might be advanced that the time-dependent functions used for extrapolation are determined solely from the signal characteristics. This conjecture is true for the cases proved here and appears to hold under less restrictive conditions. If the extrapolator functions are found by the method described, the effects of approximations inevitably introduced in the construction of optimum systems can be assessed

[11] L. A. Zadeh and J. R. Ragazzini, "An extension of Wiener's theory of prediction," *J. Appl. Phys.*, vol. 21, pp. 645–655; July, 1950.

readily. Although a completely general solution to the problem of optimum prediction still is lacking, the techniques for the design of optimum extrapolators may provide considerable insight into many previously unsolved cases and may aid in establishing rules for further understanding of optimum processes. The discussion is clarified by the following example.

Example 1

The configuration for a typical prediction system is obtained by assigning the following values:

$$\gamma_{IS-IS}(t_1, t_1+\tau) = \phi_{IS-IS}(\tau) = \pi A\delta(\tau)$$
$$\gamma_{NN}(t_1, t_1+\tau) = \phi_{NN}(\tau) = \pi a\delta(\tau)$$
$$v(t, t_1) = (t - t_1)e^{-\beta(t-t_1)}. \quad (49)$$

This impulse response corresponds to a signal-shaping network described by

$$\ddot{x}_S + 2\beta\dot{x}_S + \beta^2 x_S = x_{IS}. \quad (50)$$

The autocorrelation function for the signal component of the input is

$$\gamma_{SS}(t_2, t) = \pi A\left(\frac{1}{4\beta^3}\right)e^{-\beta|t-t_2|}(\beta|t-t_2| + 1). \quad (51)$$

Through the use of (66), the impulse response of the forward path of the optimum filter is obtained readily as

$$\pi A\left(\frac{1}{4\beta^3}\right)e^{-\beta(t-t_2)}[\beta(t-t_2)+1] = \pi a y(t, t_2),\ t > t_2. \quad (52)$$

By means of (66), the solution to (7) has been circumvented through choice of the unity-feedback configuration. The differential equation corresponding to this impulse response is

$$\ddot{x}_R + 2\beta\dot{x}_R + \beta^2 x_R = \frac{A}{a}\left(\frac{1}{4\beta^3}\right)(\dot{x}_E + 2\beta x_E), \quad (53)$$

a relation that can be derived by various techniques from (52). It is significant to note that the differential operator on the left-hand member of (53) is identical with the differential operator of (50). The integral (63) for $g(t_1)$,[12] the closed-loop impulse response, can be written

$$g(t_1) = y(t_1) - \int_0^{t_1} y(t_1 - t_2)g(t_2)dt_2. \quad (54)$$

The solution to this equation, for

$$y(t_1) = \frac{A}{a}\left(\frac{1}{4\beta^3}\right)e^{-\beta t_1}(\beta t_1 + 1), \quad (55)$$

can be found directly, but the easiest method for solving this Volterra integral equation of the second kind is to write the corresponding differential

[12] Because the filter has constant coefficients, the impulse response is written as a function of a single variable.

$$\ddot{x}_R + \left[2\beta + \frac{A}{a}\left(\frac{1}{4\beta^3}\right)\right]\dot{x}_R + \left(\beta^2 + \frac{A}{2a\beta^2}\right)x_R$$
$$= \frac{A}{a}\left(\frac{1}{4\beta^3}\right)(\dot{x}_I + 2\beta x_I). \quad (56)$$

A re-examination of (51) indicates that the forward path consists of the three parts indicated in the text: 1) a gain A/a, 2) a matching network $(1/4\beta^3)(s+2\beta)$, and 3) a model of the signal shaping network.

The functions required for the prediction operation, as indicated by (38), are

$$f_0(\tau, t) = e^{-\beta(\tau-t)}[1 + \beta(\tau - t)]$$
$$f_1(\tau, t) = e^{-\beta(\tau-t)}(\tau - t)$$
$$g_0(\tau, t) = \frac{A}{4a\beta^3}e^{-\beta(\tau-t)}(\tau - t). \quad (57)$$

Verification of these functions is obtained by partial differentiation of (38) with respect to t while τ is held constant. From (43) the extrapolator for prediction at any nonnegative number of seconds α in the future is

$$x_{RP} = e^{-\beta\alpha}\left[\alpha\dot{x}_R + (1+\beta\alpha)x_R - \frac{A\alpha}{4a\beta^3}x_E\right]. \quad (58)$$

The extrapolator for prediction at a specific fixed future instant T is

$$x_{RP} = e^{-\beta(T-t)}\left\{(T-t)\dot{x}_R + [1+\beta(T-t)]x_R - \frac{A}{4a\beta^3}(T-t)x_E\right\}. \quad (59)$$

The use of (58) with (53) yields the optimum predictor transfer function

$$\frac{x_{RP}}{x_I} = \frac{\frac{A}{4a\beta^3}e^{-\alpha\beta}[(1+\alpha\beta)s + \beta(2+\alpha\beta)]}{s^2 + \left(2\beta + \frac{A}{4a\beta^3}\right)s + \beta^2 + \frac{A}{2a\beta^2}}, \quad (60)$$

which agrees with results obtained by conventional methods.

An analog-computer setup for this problem is shown in Fig. 4, where β has been allowed to approach zero in order to simplify equipment requirements. Although the filter shown is not strictly an optimum, the optimum is broad and the chosen configuration permits the merit of the method to be assessed more quickly.

In Fig. 5, the typical results of an analog-computer study are shown for prediction at the fixed instant $T=20$ seconds. The function $x_{IS}(t)$ consists of an impulse in the presence of white noise. The signal component of the input x_S is shown on the first oscillograph record. The problem is to determine the value of x_S at the time $T=20$ seconds when the filter input $x_I(t)$ is corrupted by white noise. The output of the optimum filter $x_R(t)$ is shown in the second record where a slight displacement

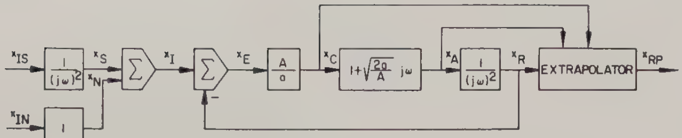

Fig. 4—Typical example of an optimum extrapolator.

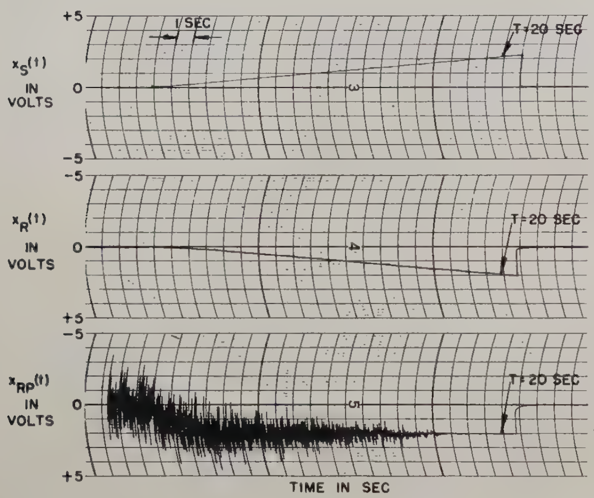

Fig. 5—Analog computer results.

or delay in the response can be detected with respect to the signal component of the input. The bottom record shows the output of the optimum extrapolator. Although the peak-to-peak amplitude of the noise is approximately 2.5 times the amplitude of the signal, $x_{RP}(t)$ rapidly assumes the correct mean value and the effects of the noise are nearly negligible over the last 3 seconds.

Appendix I

In Section II, it was stated that the integral (16) must be neglected in determining future input values. This conclusion is given greater validity in the following argument.

The definition (10) of the optimum filter allows (13) to be written as the difference of two integrals:

$$x_R(t) = \int_{-\infty}^{t} y(t, t_2)x_I(t_2)dt_2 - \int_{-\infty}^{t}\int_{-\infty}^{t_1} y(t, t_1)g(t_1, t_2)x_I(t_2)dt_2dt_1. \quad (61)$$

An interchange in the order of integration on the second integral permits the integrals to be recombined as one relation:

$$\begin{aligned} x_R(t) &= \int_{-\infty}^{t} y(t, t_2)x_I(t_2)dt_2 - \int_{-\infty}^{t}\left[\int_{-\infty}^{t} y(t, t_1)g(t_1, t_2)dt_1\right]x_I(t_2)dt_2 \\ &= \int_{-\infty}^{t}\left[y(t, t_2) - \int_{t2}^{t} y(t, t_1)g(t_1, t_2)dt_1\right]x_I(t_2)dt_2. \quad (62)\end{aligned}$$

Because this expression is the same as (10), the identity between impulse responses can be determined

$$g(t, t_2) = y(t, t_2) - \int_{t2}^{t} y(t, t_1)g(t_1, t_2)dt_1, \quad (63)$$

an equation with a well-known counterpart in the theory of time-invariant systems.[5] When both sides of (61) are multiplied by $x_I(t_3)$ and averaged,

$$\begin{aligned}\gamma_{IR}(t_3, t) &= \int_{-\infty}^{t} y(t, t_2)\gamma_{II}(t_3, t_2)dt_2 - \int_{-\infty}^{t}\int_{-\infty}^{t_2} y(t, t_2)g(t_2, t_1)\gamma_{II}(t_3, t_1)dt_1dt_2 \\ &= \int_{-\infty}^{t} y(t, t_2)\gamma_{II}(t_3, t_2)dt_2 - \int_{-\infty}^{t} y(t, t_2)\gamma_{SS}(t_3, t_2)dt_2 \\ &= \int_{-\infty}^{t} y(t, t_2)\gamma_{NN}(t_3, t_2)dt_2. \quad (64)\end{aligned}$$

The transition between the first and second equalities follows from the use of (7). Because the filter is optimum

$$\gamma_{IR}(t_3, t) = \gamma_{SS}(t_3, t), \qquad t > t_3, \quad (65)$$

and

$$\gamma_{SS}(t_3, t) = \int_{-\infty}^{t} y(t, t_2)\gamma_{NN}(t_3, t_2)dt_2, \qquad t > t_3. \quad (66)$$

This equation frequently leads to an easy interpretation of the optimum system, particularly when the noise component of the input is white. This integral equation frequently is much easier to solve than (7), and the configuration of Fig. 1 was chosen in anticipation of the result.

If (14) is hypothesized to describe the predictor response, then, by use of (65),

$$\begin{aligned}\gamma_{I-RP}(t_2, t) &= \int_{-\infty}^{t} y(t+\alpha, t_1)\gamma_{IE}(t_2, t_1)dt_1 \\ &= \int_{-\infty}^{t} y(t+\alpha, t_1)\gamma_{II}(t_2, t_1)dt_1 - \int_{-\infty}^{t} y(t+\alpha, t_1)\gamma_{IR}(t_2, t_1)dt_1 \\ &= \int_{-\infty}^{t} y(t+\alpha, t_1)\gamma_{NN}(t_2, t_1)dt_1. \quad (67)\end{aligned}$$

When t is replaced by $t+\alpha$ in (66) and comparison is made with (67),

$$\gamma_{I-RP}(t_2, t) = \gamma_{SS}(t_2, t+\alpha) - \int_{t}^{t+\alpha} y(t+\alpha, t_1)\gamma_{NN}(t_2, t_1)dt_1. \quad (68)$$

When the noise component of the input is white, the latter integral vanishes,

$$\gamma_{I-RP}(t_2, t) = \gamma_{SS}(t_2, t+\alpha). \quad (69)$$

Hence, by extending (63) the impulse response

$$h(t, t_2) = y(t + \alpha, t_2) - \int_{t_2}^{t} y(t + \alpha, t_1)g(t_1, t_2)dt_1, \quad t > t_2, \tag{70}$$

can be introduced into (11) which becomes, by reason of (12),

$$x_{RP}(t) = \int_{-\infty}^{t} y(t + \alpha, t_1)x_I(t_1)dt_1 - \int_{-\infty}^{t} y(t + \alpha, t_1)x_R(t_1)dt_1$$
$$= \int_{-\infty}^{t} y(t + \alpha, t_1)x_E(t_1)dt_1. \tag{71}$$

Eq. (71) provides a completely general relation between the response of the optimum predictor and the error signal of the optimum filter in terms of the impulse response of the forward path of the optimum filter, whenever the noise component of the input is white.

Appendix II

In Section IV the statement is made that, if the noise component of the input is white, the error signal in the optimum filter has the same autocorrelation function. The proof of this contention is fundamental to the logical discussion of the validity of the extrapolationa technique.

The autocorrelation function of the error signal is

$$\gamma_{EE}(t_1, t_2) = \overline{x_E(t_1)x_E(t_2)}$$
$$= \overline{[x_I(t_1) - x_R(t_1)][x_I(t_2) - x_R(t_2)]}. \tag{72}$$

If $g(t, t_3)$ is the impulse response of the optimum filter defined by

$$x_R(t) = \int_{-\infty}^{t} g(t, t_3)x_I(t_3)dt_3, \tag{73}$$

then $g(t, t_3)$ satisfies the integral equation for $t > t_1$

$$\gamma_{SS}(t_1, t) = \int_{-\infty}^{t} g(t, t_3)\gamma_{II}(t_1, t_3)dt_3. \tag{74}$$

As a result of the use of (73) in (72), then for $t_2 > t_1$,

$$\gamma_{EE}(t_1, t_2) = \gamma_{II}(t_2, t_1) - \int_{-\infty}^{t_1} g(t_1, t_3)\overline{x_I(t_3)x_I(t_2)}dt_3$$
$$- \int_{-\infty}^{t_2} g(t_2, t_3)\overline{x_I(t_1)x_I(t_3)}dt_3$$
$$+ \int_{-\infty}^{t_1} g(t_1, t_3) \int_{-\infty}^{t_2} \overline{x_I(t_3)x_I(t_4)}g(t_2, t_4)dt_3dt_4$$
$$= \gamma_{II}(t_1, t_2) - \int_{-\infty}^{t_2} g(t_2, t_3)\gamma_{II}(t_1, t_3)dt_3$$
$$- \int_{-\infty}^{t_1} g(t_1, t_3)\left[\gamma_{II}(t_2, t_3) - \int_{-\infty}^{t_2} g(t_2, t_4)\gamma_{II}(t_3, t_4)dt_4\right]dt_3. \tag{75}$$

Because the signal and noise are assumed to be uncorrelated,

$$\gamma_{II}(t_1, t) = \gamma_{SS}(t_1, t) + \gamma_{NN}(t_1, t), \tag{76}$$

and (74) can be written, for $t > t_1$,

$$\gamma_{NN}(t_1, t) = \gamma_{II}(t_1, t) - \int_{-\infty}^{t} g(t, t_2)\gamma_{II}(t_1, t_2)dt_2. \tag{77}$$

Thus, the right-hand side of (75) becomes, for $t_2 > t_1$,

$$\gamma_{EE}(t_1, t_2) = \gamma_{NN}(t_1, t_2) - \int_{-\infty}^{t_1} g(t_1, t_3)\gamma_{NN}(t_2, t_3)dt_3. \tag{78}$$

If the autocorrelation function of the noise is

$$\gamma_{NN}(t_1, t_1 + \tau) = \phi_{NN}(\tau) = a\delta(\tau), \tag{79}$$

then, for $\tau > 0$.

$$\gamma_{EE}(t_1, t_1 + \tau) = \phi_{NN}(\tau) - \int_{-\infty}^{t_1} g(t_1, t_3)\phi_{NN}(t_1 + \tau - t_3)dt_3$$
$$= \phi_{NN}(\tau) - ag(t_1, t_1 + \tau). \tag{80}$$

However, the last term is zero because the impulse response $g(t, t_1)$ is zero for $t_1 > t$. Hence,

$$\gamma_{EE}(t_1, t_1 + \tau) = \phi_{EE}(\tau) = \phi_{NN}(\tau). \tag{81}$$

PGAC TRANSACTIONS Reviewers

The following names constitute the list of TRANSACTIONS reviewers who have devoted considerable time to reading and criticizing preliminary TRANSACTIONS papers. Their opinions have had a direct bearing on the quality and content of the TRANSACTIONS.

We would like to extend this list, not only to relieve the burden imposed on the present reviewers, but to obtain a broader viewpoint from a larger group of control engineers. Anyone wishing to review papers in his special field should contact the editor, give his name, address, and his special interest in automatic control.

EDITOR

George S. Axelby, Air Arm Division, Westinghouse Electric Corp., Box 746, Baltimore, Md.

REVIEWERS

M. R. Aaron
E. Arthurs
J. Bacon
G. A. Biernson
J. F. Buchan
A. G. Buckingham
N. H. Chosky
E. Eckhardt
R. L. Edwards, Jr.
D. H. Evans
H. Freeman
J. E. Gibson
A. J. Groszer
V. B. Haas
A. M. Hopkin
R. E. Horn
E. I. Jury
J. Kukel
M. A. Lange
C. T. Leondes
H. Levenstein
D. P. Lindorff
M. V. Mathews
G. J. Murphy
J. A. Narud
R. D. Ormsby
W. A. Ostaff
R. H. Plath
J. M. Salzer
P. M. Schultheiss
O. J. M. Smith
P. G. Spink
C. W. Steeg
T. M. Stout
F. B. Tuteur
M. W. J. Wachter
L. B. Wadel
R. Wilcox
M. I. Witow
L. A. Zadeh
F. Zweig